Supporting information

Exceptionally Rapid Oxime and Hydrazone Formation Promoted by Catalytic Amine Buffers with Low Toxicity

Dennis Larsen, Anna M. Kietrys, Spencer A. Clark, Hyun Shin Park, Andreas Ekebergh, and Eric T. Kool*

Department of Chemistry, Stanford University, Stanford, CA 94305, United States of America

Table of Contents:

Table S1: Second-order rate constants ($M^{-1}s^{-1}$) for the reaction of phenylhydrazine and benzaldehyde at pH 7.4 using various buffers (10 – 500 mM) in saline (150 mM NaCl) and water at ambient temperature with standard deviations based on triplicate measurements.

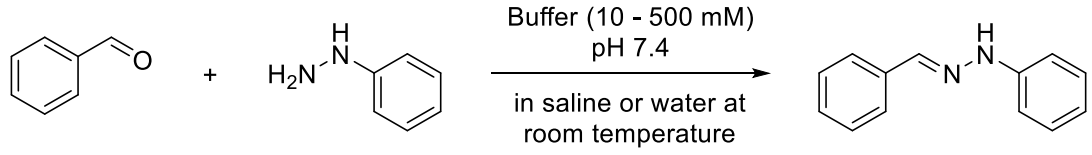

20 μM + 1.0 mM

Buffer		Buffer concentration				
		In saline			In water	
		10 mM	25 mM	50 mM	50 mM	500 mM
Phosphate	1	0.21 ± 0.02*	---	0.466 ± 0.007	---	---
Tris	2	---	---	0.481 ± 0.002	---	---
HEPES	3	---	---	0.28 ± 0.02	---	---
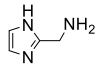	4	4.64 ± 0.18	6.0 ± 0.3	10.6 ± 0.6	9.5 ± 0.3	33.6 ± 1.0
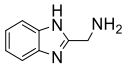	5	2.61 ± 0.06	4.60 ± 0.18	8.6 ± 0.9	8.3 ± 0.3	---
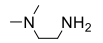	6	4.27 ± 0.12	7.3 ± 0.2	10.7 ± 0.5	6.30 ± 0.18	---
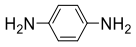	7	4.08 ± 0.18	7.5 ± 0.4	8.0 ± 0.5	9.1 ± 0.4	---
	8	---	---	0.222 ± 0.004	---	---
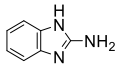	9	---	---	0.304 ± 0.004	0.352 ± 0.009	---
	10	---	---	0.216 ± 0.013	---	---
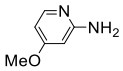	11	---	---	0.335 ± 0.010	---	---
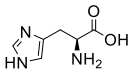	12	---	---	2.15 ± 0.02	2.02 ± 0.15	---
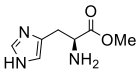	13	---	---	2.77 ± 0.06	---	---
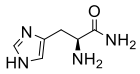	14	---	---	2.26 ± 0.02	---	---
	15	---	---	0.34 ± 0.02	0.45 ± 0.03	---
	16	0.51 ± 0.04	---	---	---	---
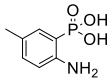	17	3.28 ± 0.12	---	---	---	---
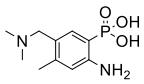	18	1.43 ± 0.05	---	2.9 ± 0.4	---	---
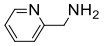	19	---	---	6.2 ± 0.2	---	---
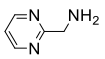	20	---	---	1.46 ± 0.04	---	---

* In 12 mM phosphate buffered saline.

Linear relationship between second-order rate constants ($M^{-1}s^{-1}$) and concentration (mM) for ABCs 4 – 7:

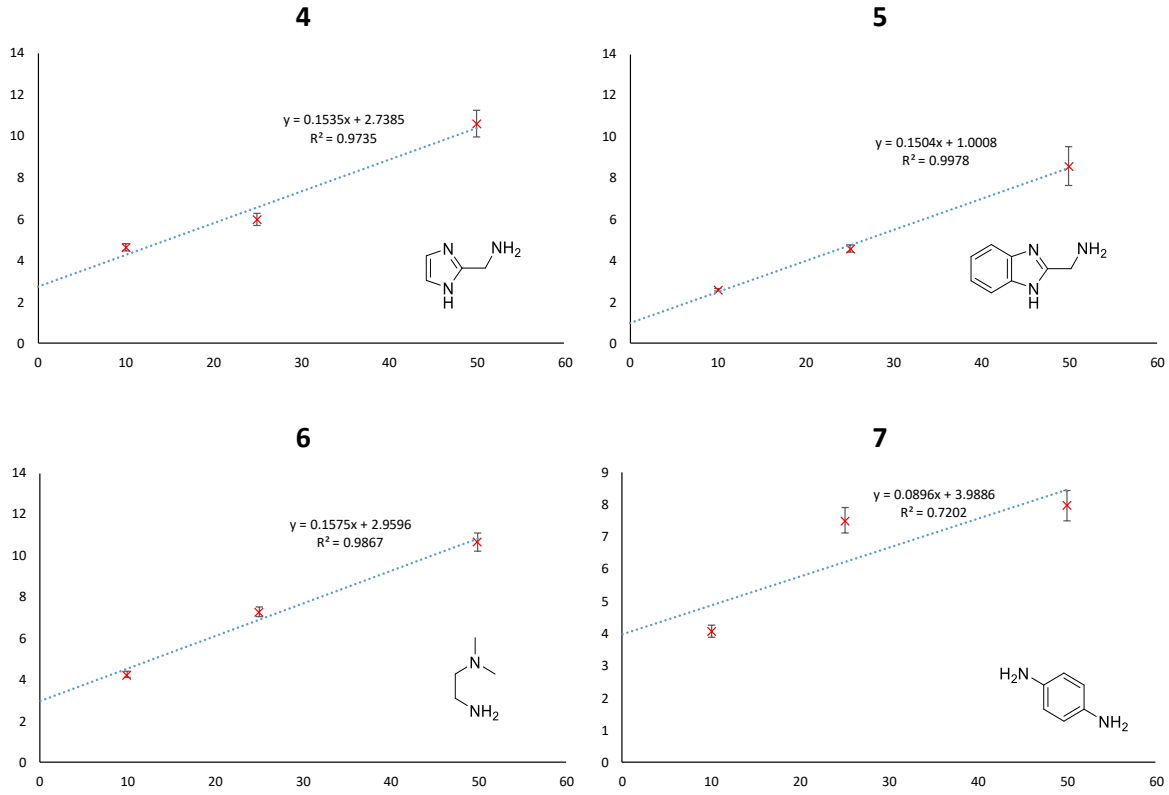

Table S2: List of buffers and their pK_a values in water at ca. 25 °C with values in biological buffering region (pK_a 6 – 9) given in red

Buffer		pK_a value(s)			Source(s)
Phosphate	**1**	2.15	7.20	12.32	R. M. C. Dawson, D. C. Elliott, W. H. Elliott and K. M. Jones
Tris	**2**		8.06		*Data for biochemical research (third edition)*, Oxford
HEPES	**3**		7.48		University Publications, Oxford, **1986**.
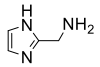	**4**	4.38[a]	8.13[a]		Potentiometric titration (see below)
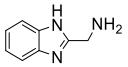	**5**		7.83		A. A. El-Sherif *J. Solution Chem.* **2010**, *39*, 1562.
	**6**		6.63	9.53	H. Irving, J. M. M. Griffiths *J. Chem. Soc.* **1954**, 213.
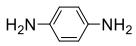	**7**	2.93	6.46		F. Mata, J. M. Leal, B. Garcia *Z. Phys. Chem.*, **1980**, *261*, 1059.
	**8**		8.46[b]		
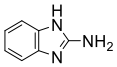	**9**		7.45		
	**10**		6.71		
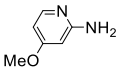	**11**		7.62		
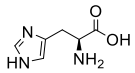	**12**	1.80	6.04	9.33	
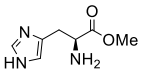	**13**	5.38	7.33		
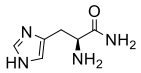	**14**	5.78	7.64		
	**15**		7.05	14.5	
	**16**	2.25	6.54	11.6	
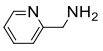	**19**	3.5	8.6		J. M. Mayer, B. Testa, *Helv. Chim. Acta* **1982**, *65*, 1868.

[a] At 23 ± 1 °C. [b] In 0.1 M KCl.

Table S3: Average second-order rate constants ($M^{-1}s^{-1}$) of the reaction between phenylhydrazine and benzaldehyde in saline (150 mM NaCl) with different buffers (50 mM) at different pH values with standard deviations based on triplicate measurements and (in italics) the relative rates vs. phosphate buffer at the same pH with compounded standard deviations

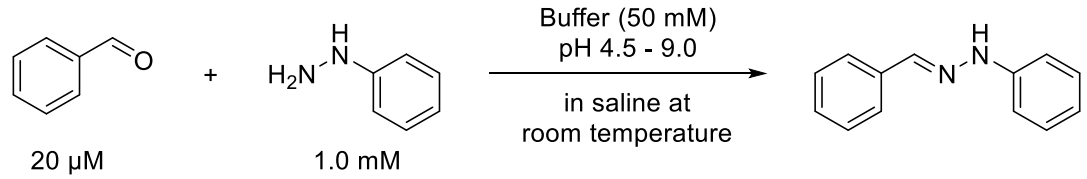

Buffer		pH 4.5	5.5	6.5	7.4	8.2	9.0
Phosphate	**1**	5.55 ± 0.19	6.0 ± 0.2	1.43 ± 0.02	0.466 ± 0.007	0.104 ± 0.002	0.054 ± 0.003
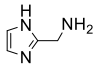	**4**	22.3 ± 0.5 *4.0 ± 0.2*	23.1 ± 0.6 *3.9 ± 0.2*	14.1 ± 0.3 *9.8 ± 0.5*	10.6 ± 0.6 *23 ± 2*	4.85 ± 0.17 *47 ± 3*	1.389 ± 0.012 *25.9 ± 1.1*
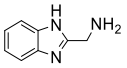	**5**	14.10 ± 0.18 *2.54 ± 0.12*	17.6 ± 0.3 *2.96 ± 0.15*	13.71 ± 0.10 *9.6 ± 0.4*	8.6 ± 0.9 *18 + 3*	2.45 ± 0.11 *23.7 ± 1.9*	0.58 ± 0.11 *10.8 ± 1.3*
	**6**	4.9 ± 1.08 *0.8 ± 0.2*	---	---	10.7 ± 0.5 *22.9 ± 1.7*	4.9 ± 0.7 *47 ± 9*	1.88 ± 0.03 *35.1 ± 1.8*
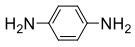	**7**	120.9 ± 1.1 *21.8 ± 0.9*	89 ± 3 *14.9 ± 1.0*	32 ± 3 *23 ± 3*	8.0 ± 0.5 *17.1 ± 1.6*	2.47 ± 0.09 *23.9 ± 1.6*	1.45 ± 0.02 *27.0 ± 1.3*

Determination of pK_a values of 4 by potentiometric titration

A calibrated pH meter was submerged into 10.0 mL of a magnetically stirred solution of **4** · 2HCl (50 mM) maintained at 23 °C. Aliquots of aq. NaOH (1.00 M) was added by use of micropipette (50 µL) and the pH was logged after it had stabilized.

A titration curve was plotted, and the best fit for a titration curve of a diprotic acid with a strong base was obtained (Figure S1).[1]

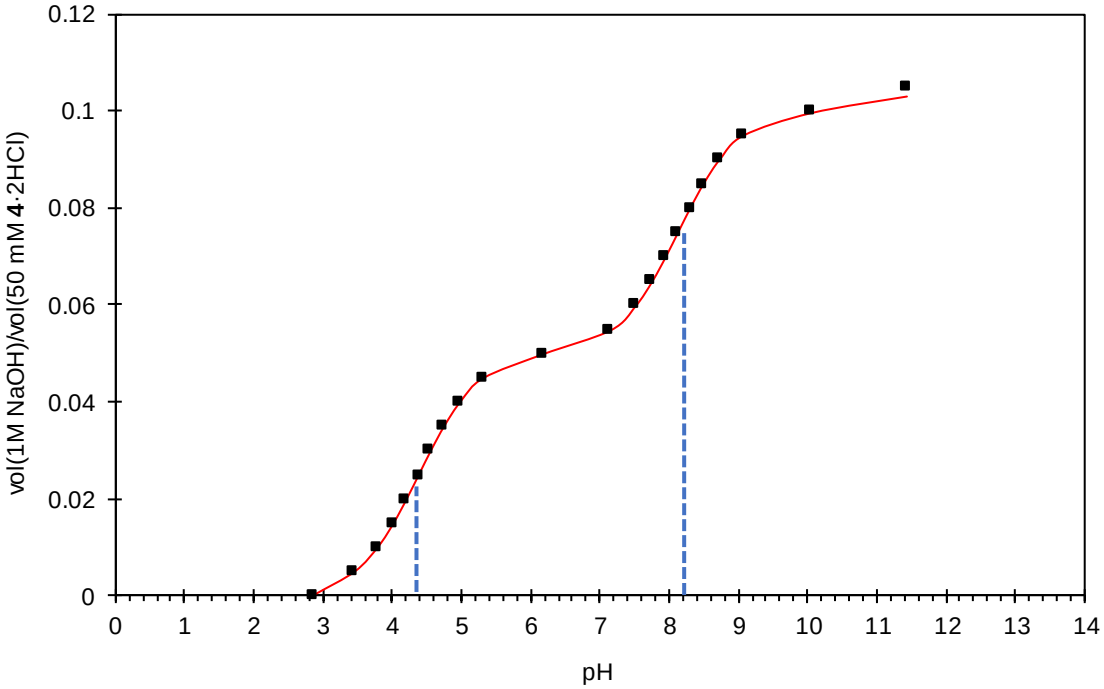

Figure S1: Titration curve of **4**·2HCl with NaOH. ▪ Experimental data point, — Best fit. Estimates of **4**'s pK_a values can be obtained from the values on the pH axis at the inflection points of the sigmoidal curves (illustrated with dashed blue lines).

The obtained fitting values are as follows:

pK_{a1} = 4.38 pK_{a2} = 8.13

Based on the relatively good fit, the error on the values are estimated to be below ±0.1 pK_a unit.

On the use of ABCs 4 – 7 in the presence of periodate

Periodate can oxidize vicinal diols or vicinal amino alcohols into aldehydes. This has been exploited to make aldehydes *in situ* on a range of biomolecules, and therefore it was investigated whether ABCs **4** – **7** could be applied in such periodate oxidation-based protocols. First, a small amount of periodate was added to buffered solutions using **4**, **5**, **6**, or **7** as the buffering agent at pH 7.4. **5**- and **7**-buffered solutions immediately turned colored, giving clear orange and clear dark red solutions respectively (Figure S2A). Upon standing, a precipitate started to form in the **5**-buffered solution, while the **7**-buffered solution turned from dark red into brown-orange (Figure S2B). No discoloration was seen with **4**- or **6**-buffered solutions.

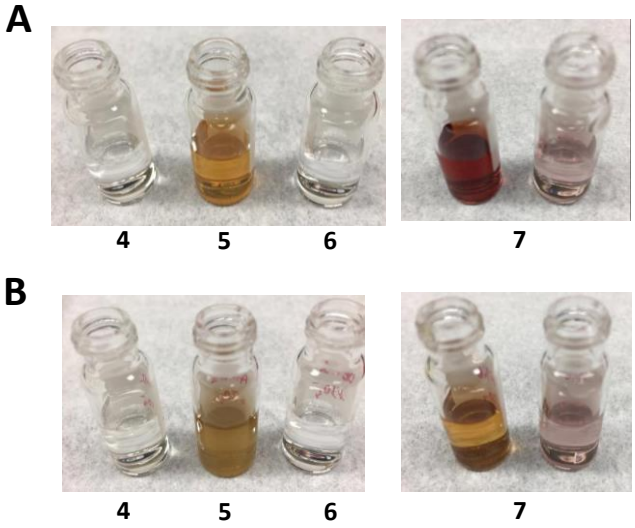

Figure S2: Photographs of solutions buffered with **4** – **7** at pH 7.4 with addition of periodate. On the far right, the pink-red coloration of a **7**-buffered solution without periodate for comparison. Solutions buffered by **4** and **6** are hard to see photographs, since both solutions are clear and colorless. A) Immediately after addition. B) Half an hour after addition. Note the precipitate in the **5**-buffered vial.

These results were taken as visual evidence that ABCs **5** and **7** are not stable to the oxidizing conditions rendered by the presence of periodate. Both **4** and **6** showed no colored products, and were applied as ABCs in the hydrazone formation of the aldehyde produced by oxidation of threonine (Thr) (Scheme S1).

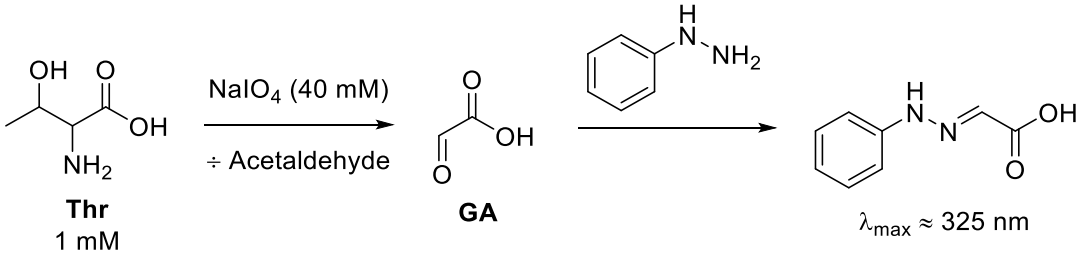

Scheme S1: The oxidation of threonine (Thr) with sodium periodate[2] produces acetaldehyde and glyoxalic aldehyde in **4**- or **6**-buffered (50 mM) saline at pH 7.4 at room temperature. The glyoxalic aldehyde (GA) reacts with phenylhydrazine to produce the hydrazone condensation product, which has an absorbance maximum at around 325 nm and thus allows for monitoring its production by UV spectrophotometry.

Firstly, the reaction was performed using GA (1 mM) and phenylhydrazine (20 µM) directly in buffers **4** or **6** (and phosphate for comparison) with buffer concetrations of 50 mM and pH at 7.4. Rise in absorbance at 325 nm was monitored to follow the progress of the reaction and non-linear regression was used to determine the second-order reaction rates (Table S4).

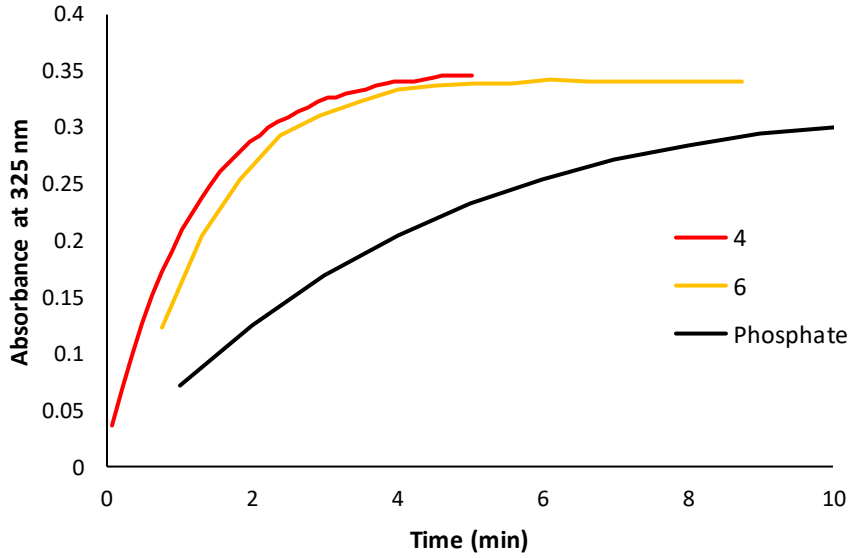

Figure S3: Change in absorbance at 325 nm as a function of time in the reaction between **GA** and phenylhydrazine in saline at room temperature buffered by the buffer indicated (50 mM) at pH 7.4.

Table S4: Average second-order rate constants for the reaction between **GA** and phenylhydrazine in saline (150 mM NaCl) at room temperature with various buffers (50 mM) with standard deviations based on triplicated measurements

Buffer		k_2 ($M^{-1}s^{-1}$)
Phosphate	**1**	4.1 ± 0.2
	**4**	12.92 ± 0.19
	**6**	12.6 ± 0.6

As is seen in Table S4, **GA** reacts with phenylhydrazine at a high rate under these conditions.

Then, the reaction was performed with threonine according to Scheme S1, allowing the threonine to oxidize for fifteen minutes with periodate before addition of phenylhydrazine. Absorbance at 325 nM was monitored to follow the progress of the reaction (Figure S4).

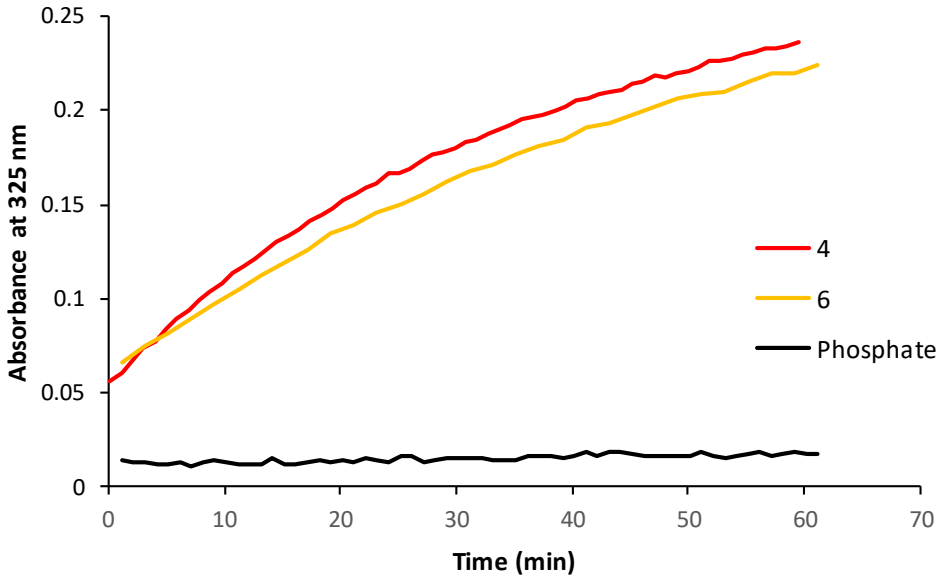

Figure S4: Change in absorbance at 325 nm as a function of time in the reaction between **Thr** and phenylhydrazine in saline with sodium periodate (40 mM) at room temperature buffered by the buffer indicated (50 mM) at pH 7.4.

As evidenced in Figure S4, the reaction rate is many orders of magnitude faster in **4**- or **6**-buffered solutions than in phosphate buffered solution. The rate of reaction with threonine is considerably slower than with **GA** indicating that the rate-limiting step (at least in **4** or **6** buffered solution) is the oxidation step preceding the condensation step. Interestingly, it is possible to get a measure for the reaction rate of the periodate-mediated oxidation of threonine in the different buffers (Table S5). By utilizing that the absorbance measurements were performed at a constant time interval and the assumption that the reaction was under pseudo-first order conditions (40-fold excess of periodate), the Guggenheim method was applied to achieve the observed first-order reaction rate, k_{obs}, and employing $k_2 = [\text{periodate}] \cdot k_{obs}$ allows for deduction of the apparent second-order rate constant, k_2. The slow rate of formation in phosphate buffer does not allow for the determination of k_2 in this instance, but for **4** and **6** excellent linearity was observed in the Guggenheim plots (Figure S5).

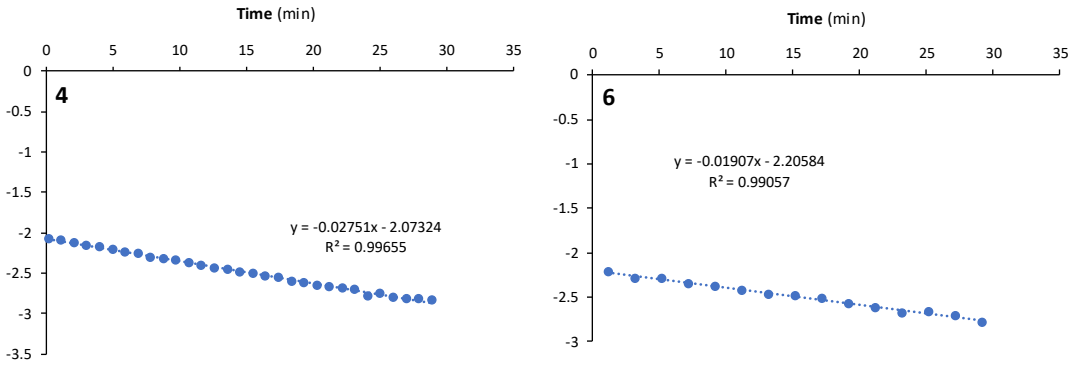

Figure S5: Guggenheim plots of the pseudo-first order reaction between **Thr** and phenylhydrazine in saline with sodium periodate (40 mM) at room temperature with the indicated buffer (50 mM) at pH 7.4. Both plots show excellent linearity. The slope gives the negative value of the observed pseudo-first order reaction rate, k_{obs}. Note that the resulting value will be in units of min^{-1} since the time axis is in units of minutes.

Table S5: Estimated second-order reaction rate for the periodate oxidation of threonine in saline at room temperature in buffer **4** (50 mM) or in buffer **5** (50 mM) with standard error on the linear fit

Buffer		k_2 ($M^{-1}s^{-1}$)
	**4**	0.459 ± 0.005
	**6**	0.318 ± 0.009

The values listed in Table S5 are similar to those reported for the periodate oxidation of pinacol at neutral pH (ca. 0.8 – 1.0 $M^{-1}s^{-1}$).[2]

Cytotoxicity assays

In total, three cell viability assays have been performed. The MTT/formazan method, which relies on spectrophotometric determination of the purple compound formazan, was used in one protocol, while a combination of resazurin/resorufin and SYTOX green, both relying on fluorescence emission but in different parts of the spectrum allowing for use in unison, was used in the other protocol. Both are commercially available assays.

The MTT/formazan assay is based on the NADH/NADPH-based reduction of a tetrazolium salt (MTT) by viable cells. The formazan product of this reduction absorbs light at 510 – 650 nm and thus the amount formed can be detected spectrophotometrically. Formazan, however, is a hydrazone and thus might be prone to hydrolysis using the ABCs in this study, which is why a fluorescence based assay was also performed.

In metabolically active cells, resazurin, which is non-fluorescent, is reduced to resorufin, which emits in the red part of the spectrum. SYTOX green is a green-fluorescent nucleic acid stain, that lights up in cells with compromised membranes. The two fluorescent probes do not overlap and can be used in unison, allowing for a measure of cell membrane permeability (SYTOX green) and cell metabolic activity (resorufin) in one well.

Protocols:

MTT/formazan assay:

1. HeLa cells were seeded at a concentration of 1.2 × 10^4 cells per well to 96-well plate in supplemented DMEM culture medium (10% FBS, 100U Pen./Strep., Gibco) and incubated for 16h at 37°C and 5% CO_2.
2. HeLa cells were incubated with 200 µM, 500 µM, 1 mM, 5 mM, 10 mM, and 20 mM of compounds **4**-**7** for 6 h at 37 °C and 5% CO_2, in supplemented DMEM culture medium. Medium was supplemented additional HEPES pH 7.4 in concentrations: 250 µM (200µM, Gibco), 625µM (500 µM), 1.25mM (1mM), 6.25mM (5mM), 12.5mM (10mM), 25mM (20mM). Control cells were incubated in the supplemented DMEM (Ctrl), and in the supplemented DMEM with 25mM HEPES pH 7.4 (Ctrl HEPES).
3. After the incubation period, 10µl of the MTT labeling reagent (final concentration 0.5 mg/ml, Roche) was added to each well, and incubated for 4 h at 37°C and 5%.
4. 100 µl of the Solubilization solution was added into each well, and incubated for 20h at 37°C and 5%.
5. Absorbance of the samples was measured using a microplate reader Tecan Infinite M1000 at 550, and 650 nm.

Resorufin and SYTOX green assay:

1. HeLa cells were seeded at a concentration of 1.4 × 10^4 cells per well to 96-well plate (black, flat transparent bottom, Greiner) in supplemented DMEM culture medium (10% FBS, 100U Pen./Strep., Gibco) and incubated for 16 h at 37°C and 5% CO_2.
2. HeLa cells were incubated with 200µM, 500 µM, 1mM, 5mM, 10mM, and 20mM of compounds 1-4 for 6h at 37°C and 5% CO_2, in supplemented DMEM culture medium. The medium was

supplemented additionally HEPES pH 7.4 (Gibco) in concentrations: 250 µM (200µM), 625µM (500 µM), 1.25mM (1mM), 6.25mM (5mM), 12.5mM (10mM), 25mM (20mM). Control cells were incubated in the supplemented DMEM (Ctrl), and in the supplemented DMEM with 25mM HEPES pH 7.4 (Ctrl HEPES).

3. After the incubation period medium was removed and 100µl fresh, not supplemented DMEM medium (without phenol red) was added to each well. Medium contained 10 nM SYTOX Green and 5 µM C12-resazurin (Thermo Fisher Scientific). Plate was incubated for 15 minutes at 37°C and 5% CO_2 in the dark.
4. Fluorescence of the samples was measured using a microplate reader Tecan Infinite M1000 at excitation 480nm, and emissions 530nm for SYTOX Green, and 575nm for resofurin.

Comments:

1. Compounds **4** – **7** were diluted to 20 mM in DMEM supplemented medium with 25 mM addition of HEPES pH 7.4. Using 20 mM sample dilutions 10 mM, 5 mM, 1 mM, 0.5 mM, and 0.2 mM were prepared in the supplemented DMEM.
2. A set of controls was prepared: Ctrl – cells cultured only in the supplemented DMEM; Ctrl HEPES - cells cultured in the supplemented DMEM with 25mM addition of HEPES to confirm no changes was caused by addition of HEPES (No significant difference was observed). Compound **7** tends to be reddish pink, so additional set of controls has been prepared: range of pDAB dilutions (20-0.2 mM) in the supplemented DMED with HEPES (the same solution that was added to the cells).
3. DMEM contains 44 mM sodium bicarbonate ($NaHCO_3$) as a buffering reagent but to increase buffer capacity addition of 25 mM HEPES pH 7.4 to 20 mM dilution has been used. Significant pH change for compounds **4**, **5**, and small for **7** has been observed. Images of dilutions below.

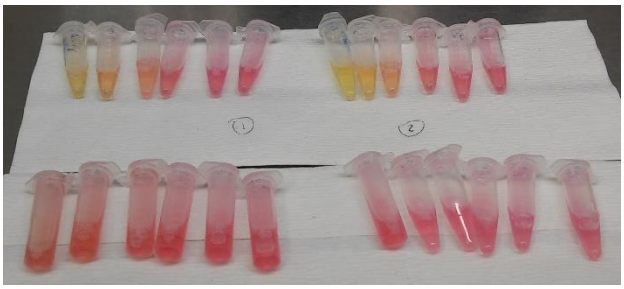

(top left: **4**, top right: **5**, bottom left, **7**, bottom right: **6**)

4. **7** tends to be reddish pink in medium (image below), and this phenomenon resulted in background absorbance for 20 mM, and 10 mM samples in the MTT/formazan assay. The background was subtracted during analysis. Images of plate below.

7 (MTT):

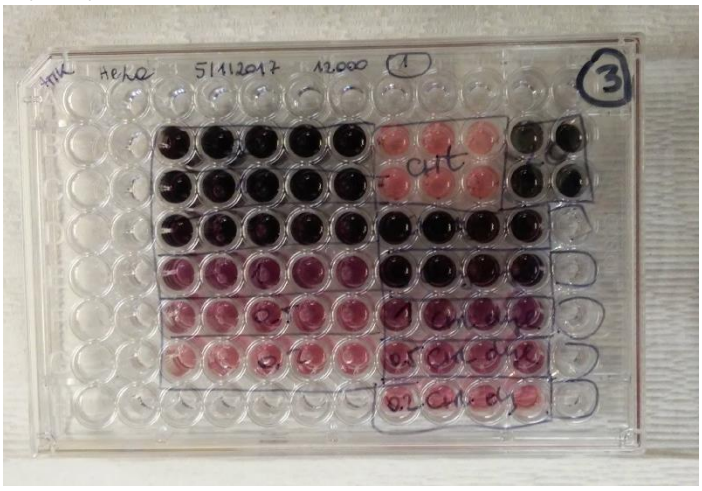

For comparison, images of plates for other compounds follow below.

4 (MTT):

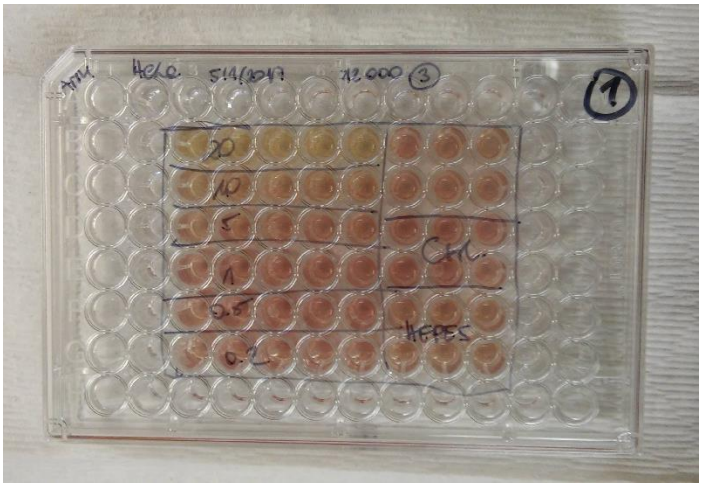

5 (MTT):

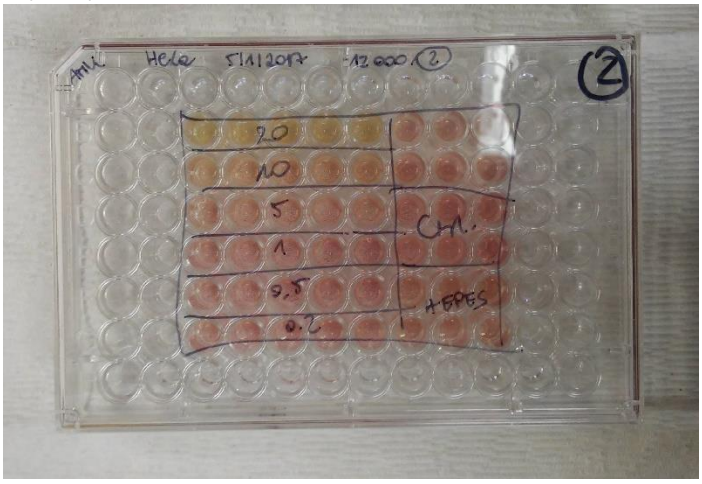

6 (MTT):

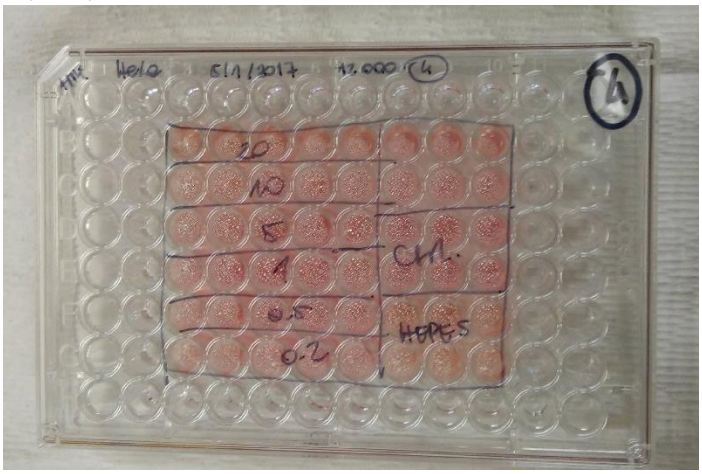

Results (Summary):

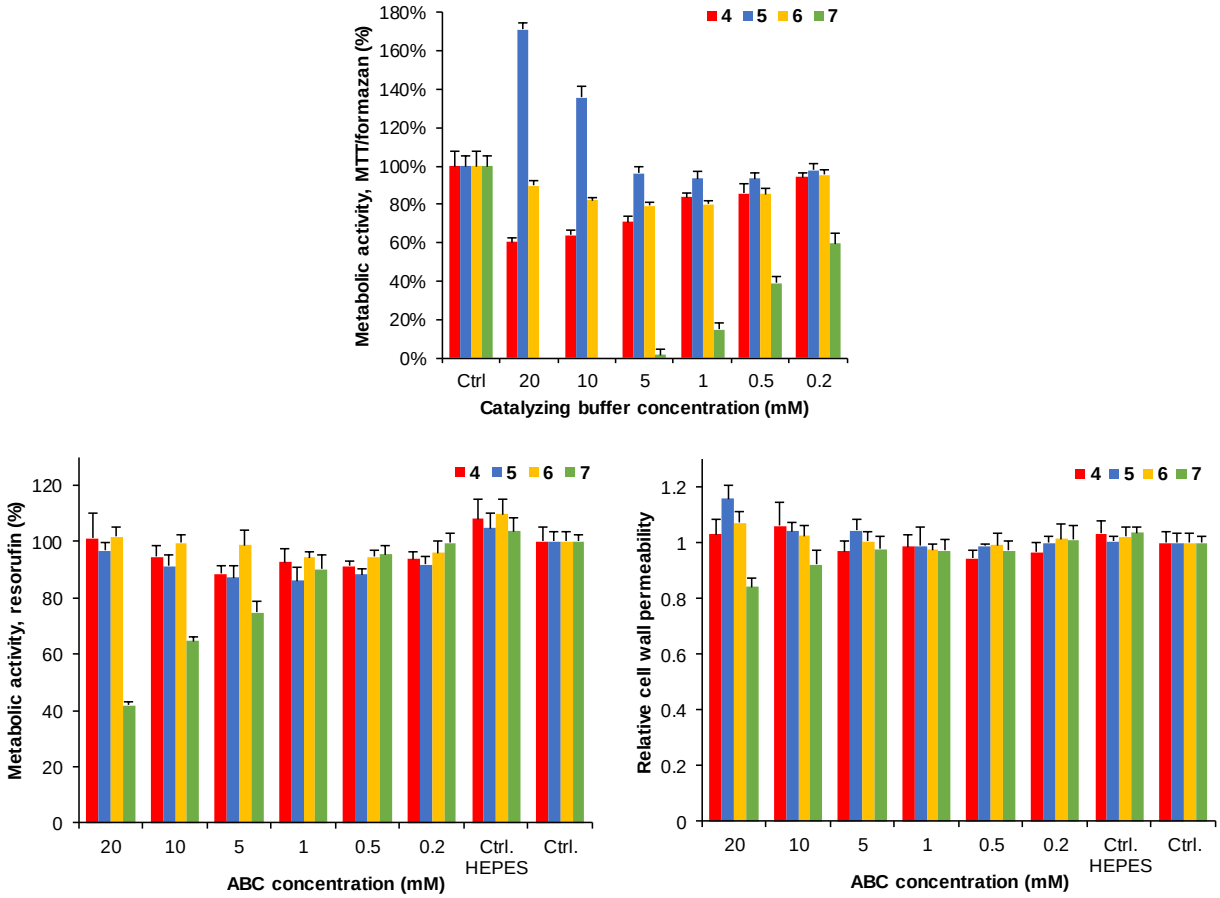

Figure S6: Summary of cytotoxicity assays. Height of bars represent mean values relative to the control experiment ("Ctrl"). Error bars are standard deviations based on measurements from five individual wells. Top: MTT/formazan UV absorbance-based metabolic activity results. Bottom: Resorufin metabolic activity (left) and SYTOX green cell wall integrity (right) fluorescence-based results.

In the MTT/Formazan assay, **7** stands out as the only compound showing significant toxicity (Figure S6, top). Compound **5** apparently results in results in an *increase* in metabolic activity, but this could be due to the compound interfering with the assay (formazan is a hydrazone, and hydrazone formation/stability is influenced by these buffers). The results of the resorufin assay are therefore considered more reliable here, and these results confirm that **7** does indeed show an increased toxicity in comparison to compounds **4** – **6** (Figure S6, bottom left). Interestingly, the SYTOX green screening indicates that the permeability of the cells is not affected to a high degree for either compound, although **7** once again stands out by apparently lowering cell permeability. This indicates that the toxicity of **7** seen in the metabolic assays does not result from rupturing of the cell membranes, or that **7** downregulates some membrane-related cellular mechanism. If the latter is the case, the observed lowering of resorufin fluorescence could be because of lower uptake of the resazurin (which should pass the membrane easily under normal conditions).

Cell-based experiments:

Coumarin quenching experiments. HeLa cells were seeded at a concentration of 2.8×10^4 cells per well to an 8-well plate in supplemented DMEM culture medium (10% FBS, Gibco, 100 U Pen./Strep., Gibco) and incubated for 16 h at 37°C and 5% CO2 with 95% humidity. Old medium was removed and replaced with 200 µL of a new supplemented DMEM medium (Gibco) containing 10 µM 7-diethylamino-3-formylcoumarin **21**. HeLa cells were incubated with the coumarin for 1 h at 37°C. Next medium was removed and cells were washed twice with 1 x PBS (Gibco). To the control wells 1 x HBSS buffer (Gibco) containing 10 mM buffer **4** or PBS (Gibco), and 50 mM HEPES pH 7.4 (Gibco) and 0.5% DMF (Thermo Fisher) was added. To trigger reaction with the coumarin in cells, 1 x HBSS buffer (Gibco) containing 10 mM buffer **4** or PBS (Gibco), and 50 mM HEPES pH 7.4 (Gibco) and 50 µM dabsyl-oxyamine **22** in DMF (Thermo Fisher) was added. HeLa cells were incubated with 1 x HBSS buffer (Gibco) for 1 h at 37°C. Next, buffer was removed, and wells were washed twice using 1 x PBS. The plates prepared for visualization using the epifluorescence microscope Nikon Eclipse i80 at room temperature. Visualization and imaging of cells were carried out using bright field and fluorescence filters 400 nm > λ_{ex} >440 nm; 560 nm > λ_{em} > 640 nm. Images were analyzed using Image J software. Resulting data is presented in Figure 5 of the manuscript. **21**[3] and **22**[4] were synthesized following protocols from the literature. Spectra were consistent with published values.

Formaldehyde imaging experiments. HeLa cells were seeded at a concentration of 2.8×10^4 cells per well to an 8-well plate in supplemented DMEM culture medium (10 % FBS, Gibco, 100 U Pen./Strep., Gibco) and incubated for 16 h at 37 °C and 5 % CO2 with 95 % humidity. The old medium was removed, and the cells were washed with 1 x PBS (Gibco). The cells were supplied with 1 x HBSS buffer containing 500 µM formaldehyde, 20 µM DarkZone probe,[5] 50mM HEPES pH 7.4 (Gibco), and 10 mM buffer **4** or PBS and incubated for 1 h at 37 °C. Next, medium was removed, and wells were washed twice using 1 x PBS. The plates were prepared for visualization using the epifluorescence microscope Nikon Eclipse i80 at room temperature. Visualization and imaging of cells were carried out using bright field and fluorescence filters 460 nm< λ_{ex} <500nm; 505 nm < λ_{em} <520 nm. Images were analyzed using Image J software. The data are presented in Figure S7 below.

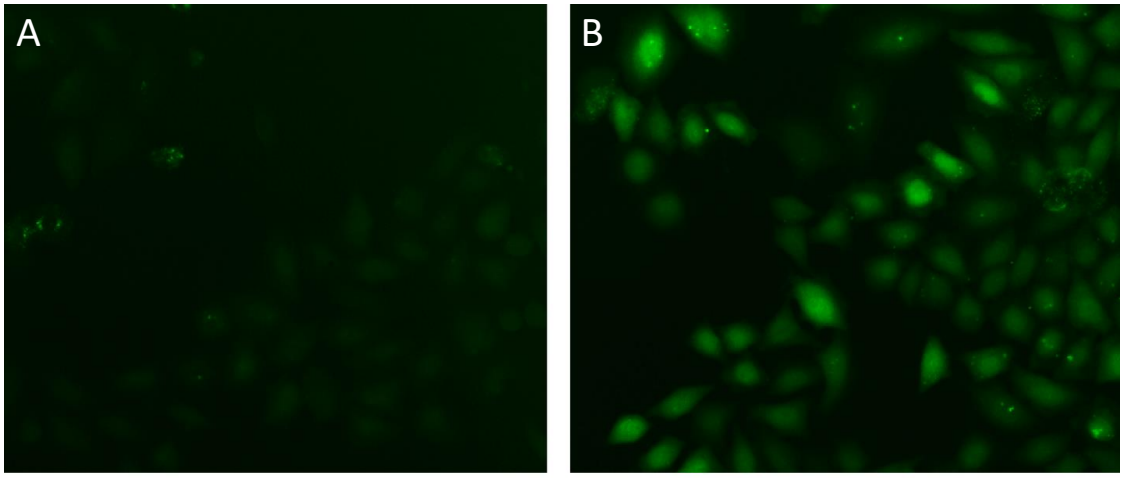

Figure S7: Imaging formaldehyde in HeLa cells by hydrazone exchange, promoted by buffer **4**. Epifluorescence microscope image of cells with formaldehyde (500 µM) and DarkZone probe (20 µM) after: (A) one hour in HBSS medium; (B) one hour in the presence of buffer **4** (10 mM) in HBSS medium.

Protein fragment labeling using Alexa Fluor 488 hydrazide

RNase A protein (75 µg, Sigma Aldrich) was partially digested by addition of 0.4 µg Subtilisin (Sigma Aldrich) in reaction buffer (20 mM phosphate buffer pH 7.6, 0.15 mM KCl, 10 mM $MgCl_2$, 5 mM DTT) for 3.5 h on ice, to produce fragments with serines at N-termini.[6] To 30 µL of the reaction mixture 28 µL of PBS (Gibco, pH 7.2), and 2 µL of sodium periodate (0.5 M in water, Sigma Aldrich) were added. The oxidation was carried out for 25 min at room temperature in the dark. Immediately, the buffer was triply exchanged to AMI (**4**) (pH 7.4, Sigma Aldrich) or PBS (pH 7.4, Gibco) using 3 kDa cutoff filters (Amicon Ultra 0.5 mL centrifugal filters, Millipore Sigma). The peptide fragments and remaining native RNase A protein were stained with Alexa Fluor 488 hydrazide (Thermo Fisher Scientific). The final reaction of 30 µL volume contained 150 µg of RNase/peptides in 10 mM PBS/**4** of pH 7.4, and 0.5 mM or 1 mM Alexa Fluor 488 hydrazide. The reaction mixture was incubated for 1 h at room temperature in the dark. Then, both protein and peptides were triply purified on 3 kDa cutoff filters using 10 mM PBS (pH 7.4) or 10 mM **4** (pH 7.4) as the exchanging buffers. The Bradford reagent (Quick Start™ Bradford Protein Assay, Bio-Rad) was used to measure concentration of peptides/proteins in the samples, according to manufacturer's protocol. 15 µg of the peptide/protein was separated in the 4 – 12 % Bis-Tris SDS gel (Thermo Fisher Scientific) for 50 min in the 1 x MES SDS running buffer (Thermo Fisher Scientific), 160 V. The gel was rocked for 0.5 h in deionized water and visualized by Typhoon 9410 Molecular Imager (GE Amersham Molecular Dynamics). In the next step, the gel was stained in Coomassie Blue R-250 (0.1 % in 40 % ethanol and 10 % acetic acid in water, Thermo Fisher) for 1 min at 96 °C. Unstaining of the gel was performed in 10 % ethanol and 7.5 % acetic acid in water for 16 h at room temperature with constant rocking. The gel was visualized using an optical camera.

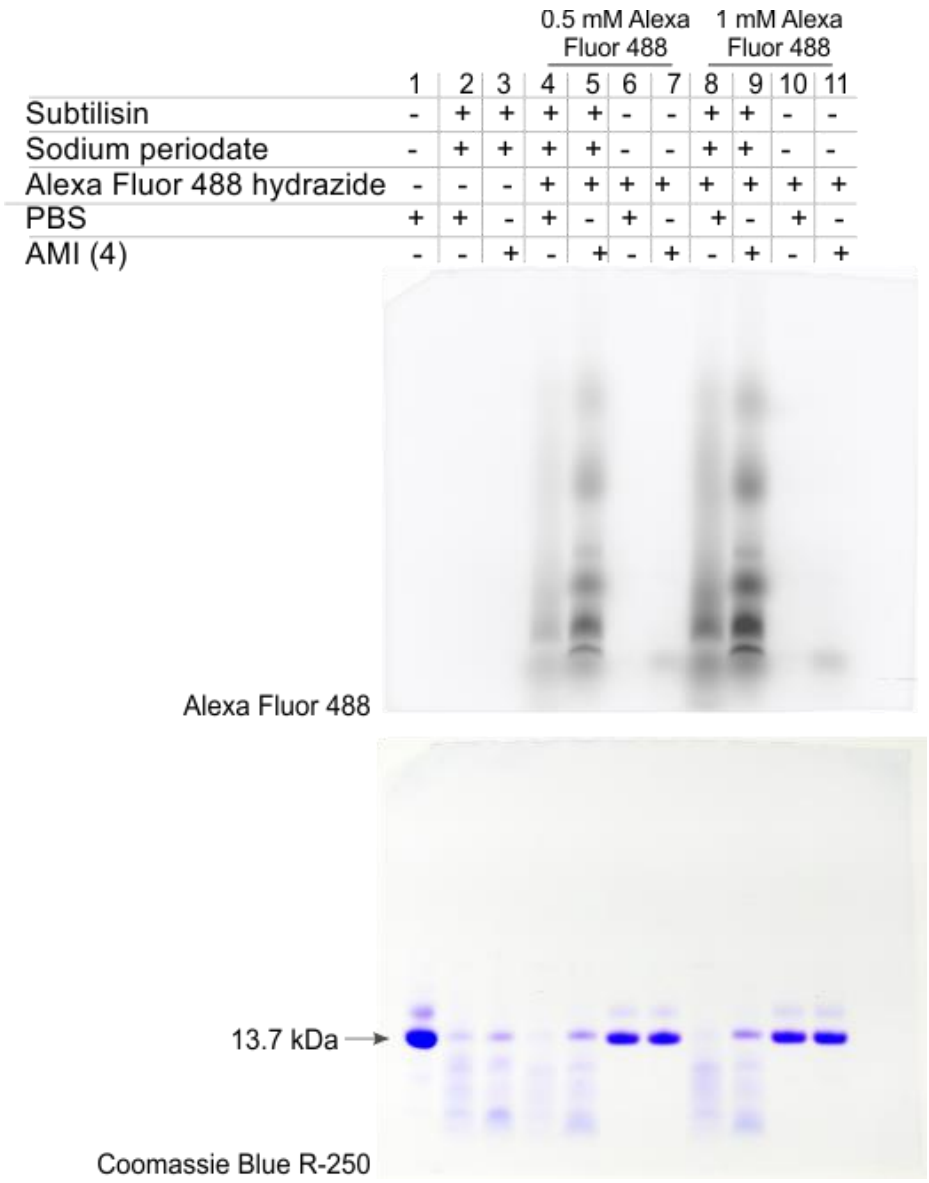

Figure S8. Increase in hydrazone formation (protein fragment staining) efficiency using AMI (**4**) as a buffering reagent. The images show the same Bis-Tris SDS gel visualized using filter for Alexa 488 (top image) and Coomassie blue R-250 (bottom image). The comparison of lanes 4 to 5 and 8 to 9 illustrates significantly higher level of labeled proteins in the lanes corresponding to hydrazone formation performed in 10 mM **4** (lane 5 and 9) as compared to 10 mM PBS (lane 4 and 8). Each lane contains 15 µg protein as measured by the Bradford assay.

Determination of second-order rate constants by non-linear regression

Representative time-resolved absorbance changes with best fits for the model reaction in saline at pH 7.4 with various buffers at 50 mM (resulting values are listed in Table 1 in the manuscript and in Table S1)

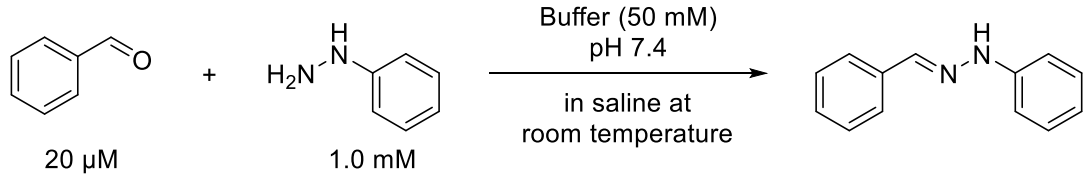

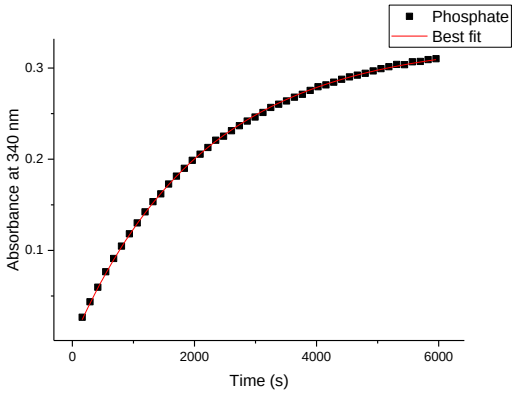

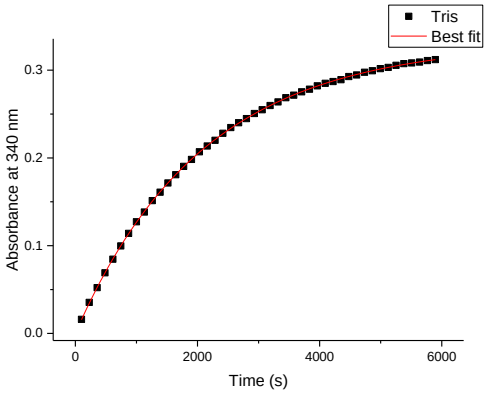

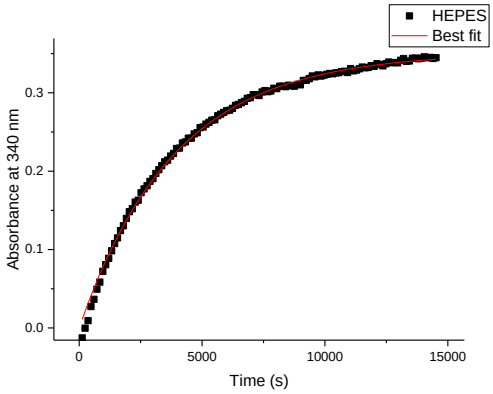

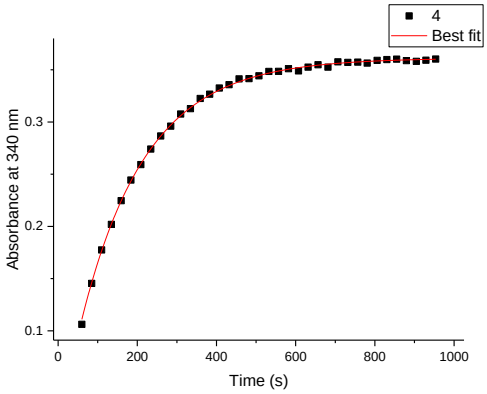

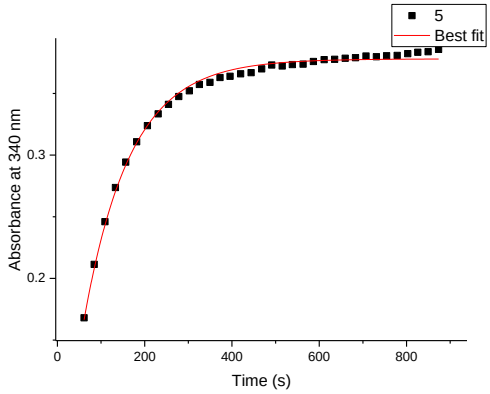

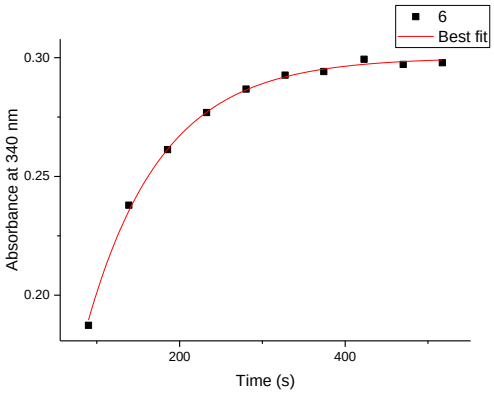

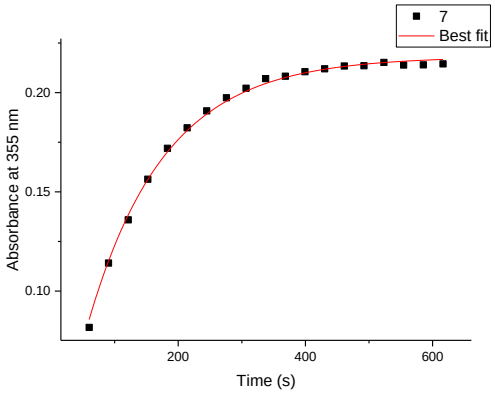
7
Best fit
Absorbance at 355 nm
Time (s)

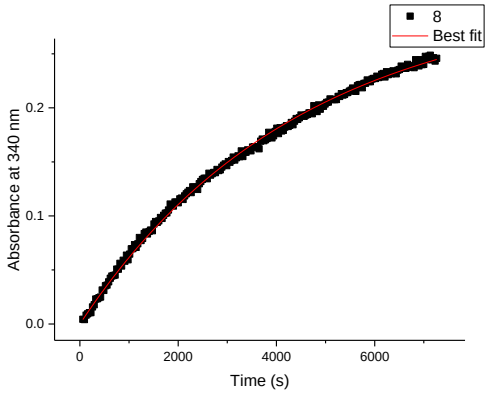
8
Best fit
Absorbance at 340 nm
Time (s)

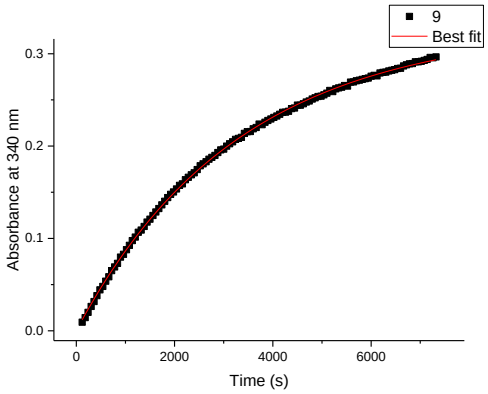
9
Best fit
Absorbance at 340 nm
Time (s)

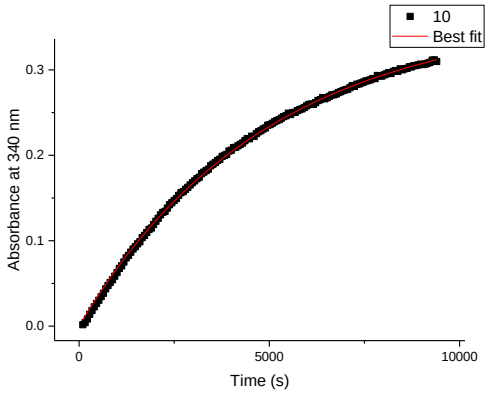
10
Best fit
Absorbance at 340 nm
Time (s)

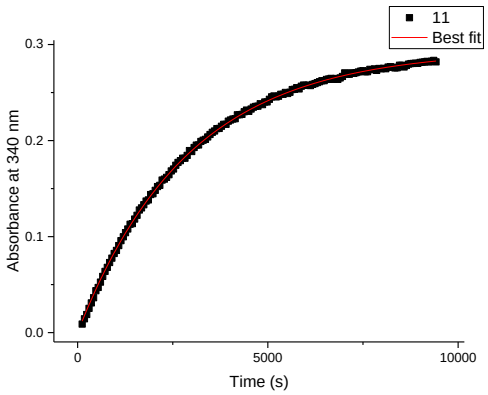
11
Best fit
Absorbance at 340 nm
Time (s)

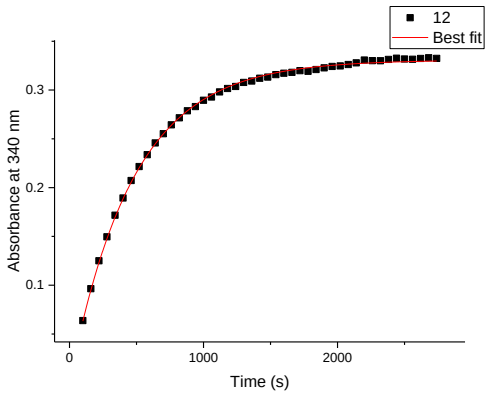
12
Best fit
Absorbance at 340 nm
Time (s)

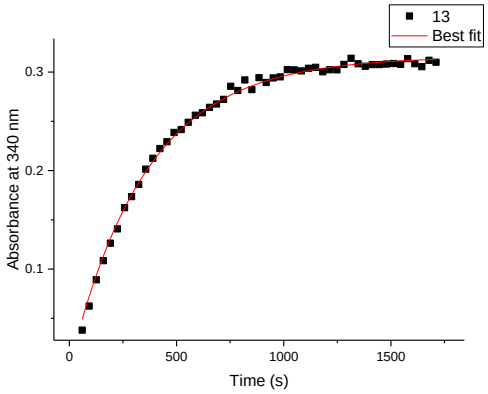
13
Best fit
Absorbance at 340 nm
Time (s)

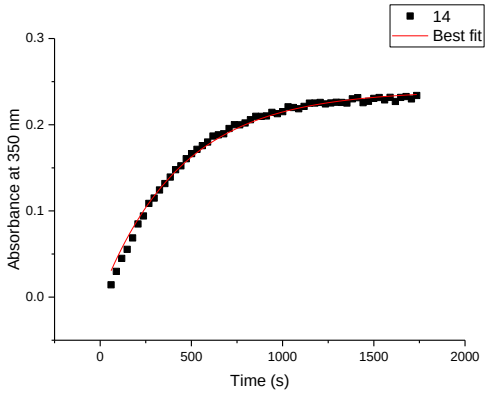
14
Best fit
Absorbance at 350 nm
Time (s)

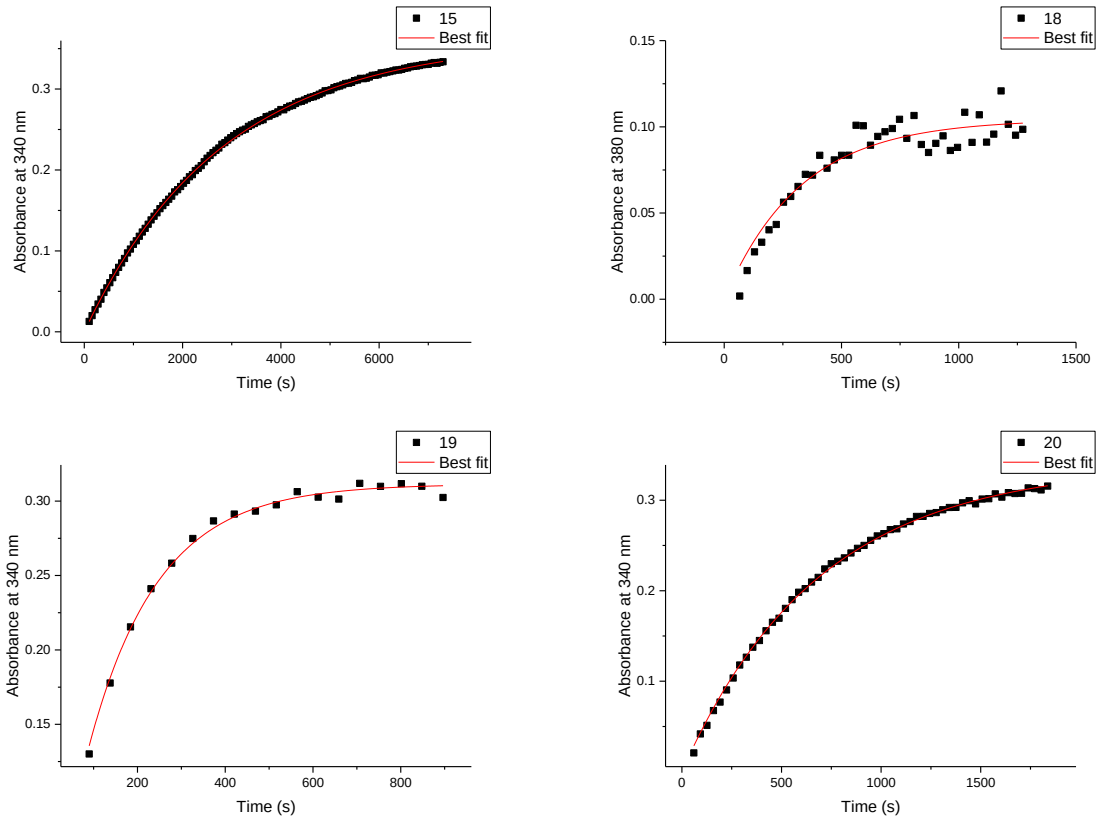

Representative time-resolved absorbance changes with best fits for the model reaction in saline or water at pH 7.4 with various buffers at 10, 25, 50, or 500 mM (resulting values are listed in Table S1)

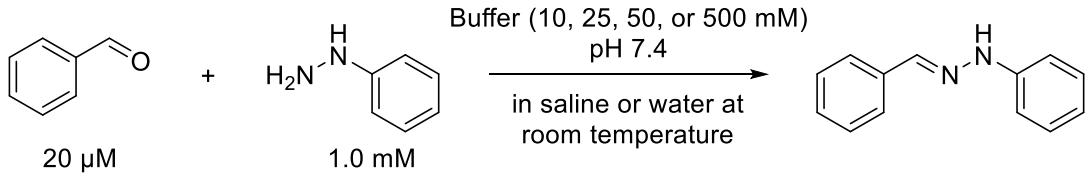

In saline:

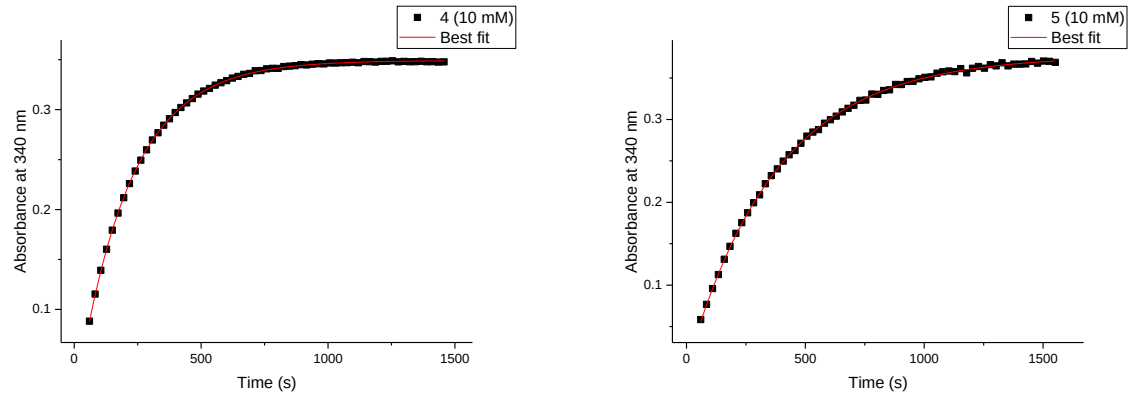

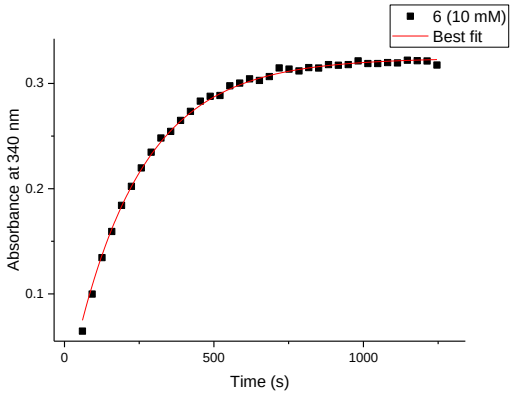
6 (10 mM)
Best fit
Absorbance at 340 nm
Time (s)

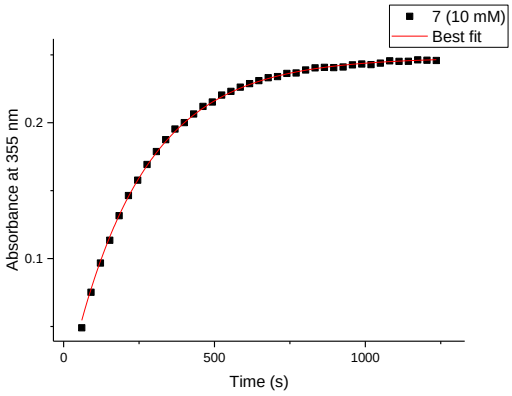
7 (10 mM)
Best fit
Absorbance at 355 nm
Time (s)

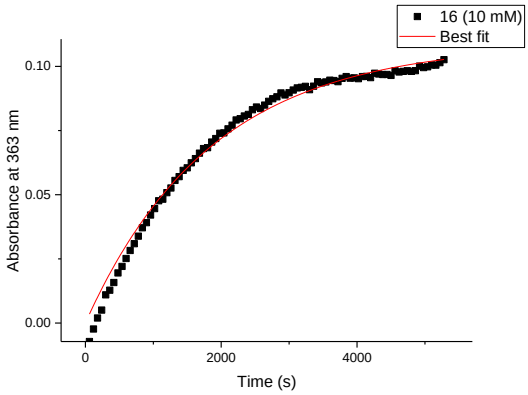
16 (10 mM)
Best fit
Absorbance at 363 nm
Time (s)

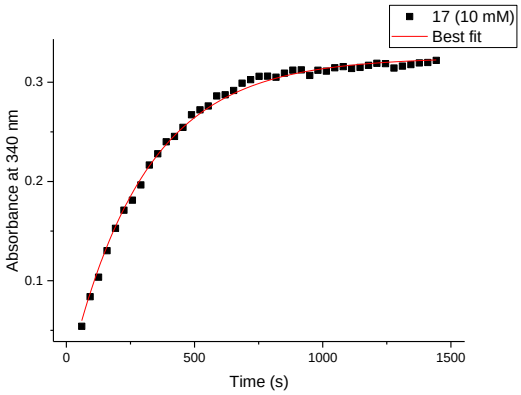
17 (10 mM)
Best fit
Absorbance at 340 nm
Time (s)

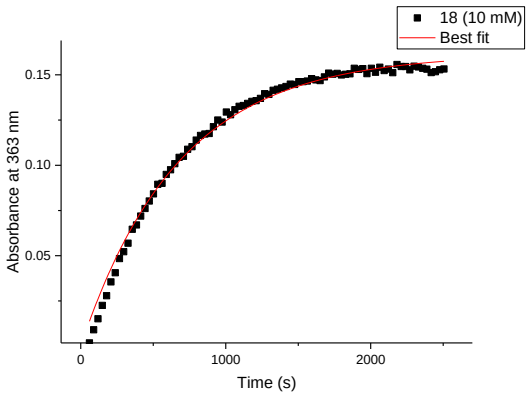
18 (10 mM)
Best fit
Absorbance at 363 nm
Time (s)

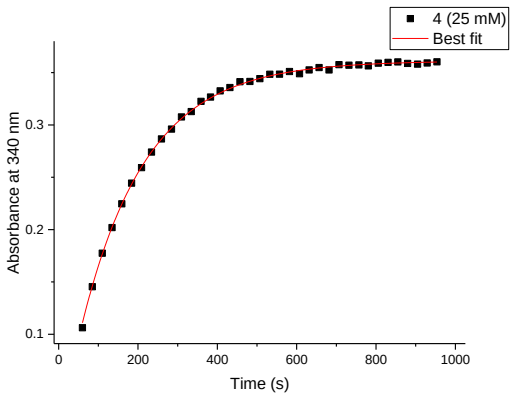
4 (25 mM)
Best fit
Absorbance at 340 nm
Time (s)

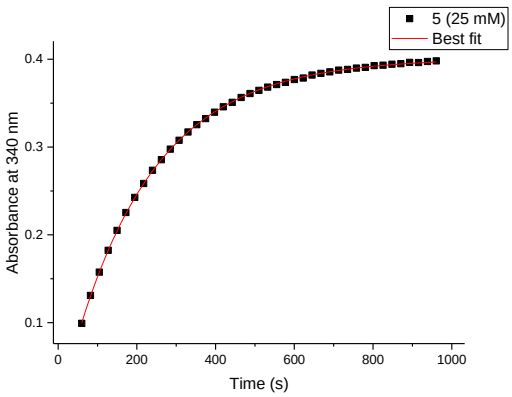
5 (25 mM)
Best fit
Absorbance at 340 nm
Time (s)

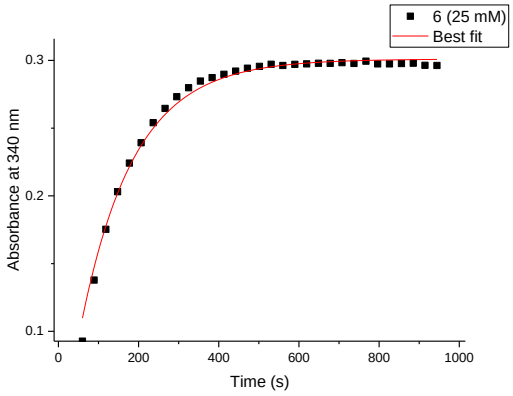
6 (25 mM)
Best fit
Absorbance at 340 nm
Time (s)

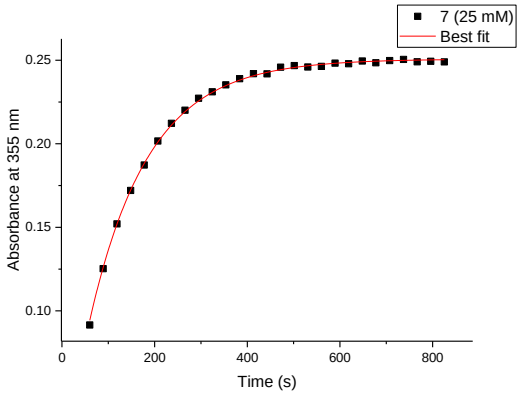
7 (25 mM)
Best fit
Absorbance at 355 nm
Time (s)

In water:

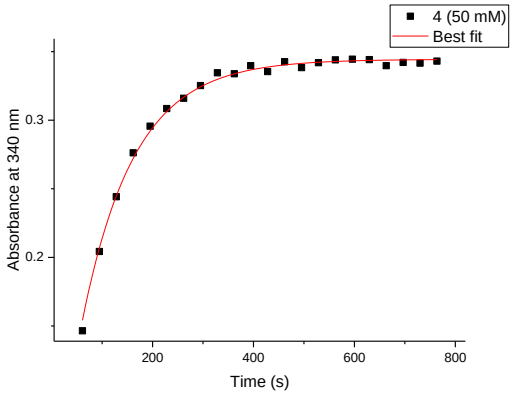
4 (50 mM)
Best fit
Absorbance at 340 nm
Time (s)

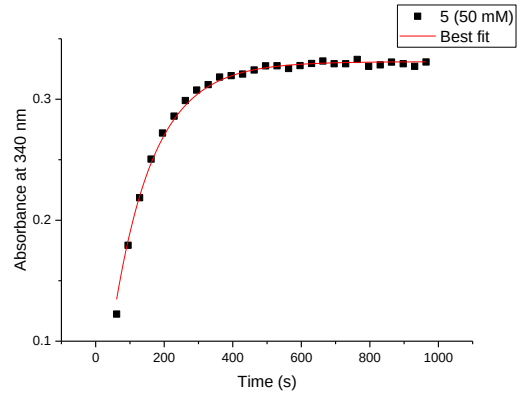
5 (50 mM)
Best fit
Absorbance at 340 nm
Time (s)

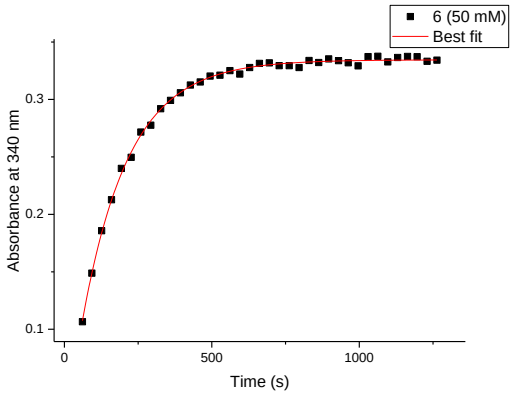
6 (50 mM)
Best fit
Absorbance at 340 nm
Time (s)

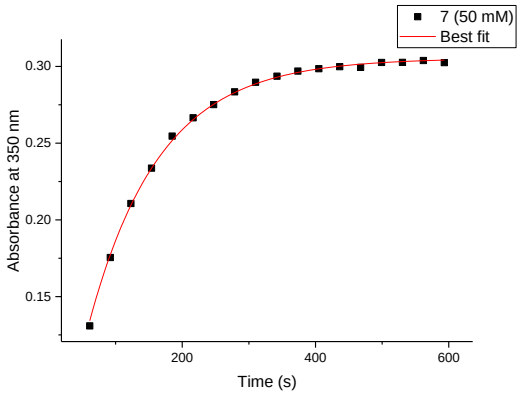
7 (50 mM)
Best fit
Absorbance at 350 nm
Time (s)

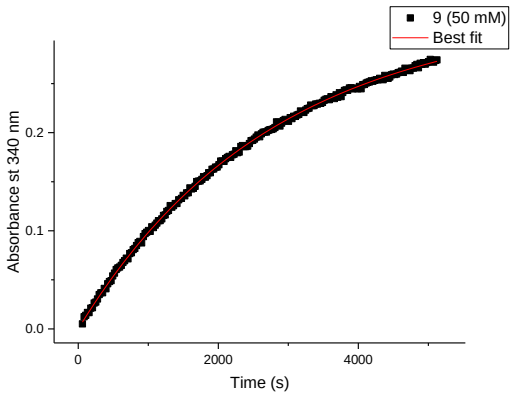
9 (50 mM)
Best fit
Absorbance st 340 nm
Time (s)

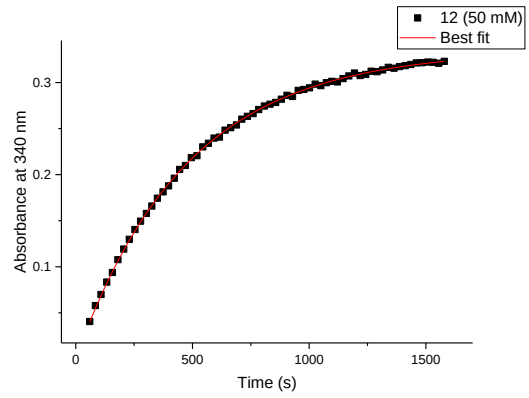
12 (50 mM)
Best fit
Absorbance at 340 nm
Time (s)

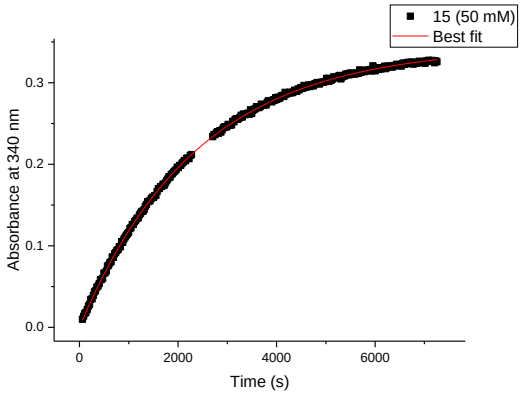

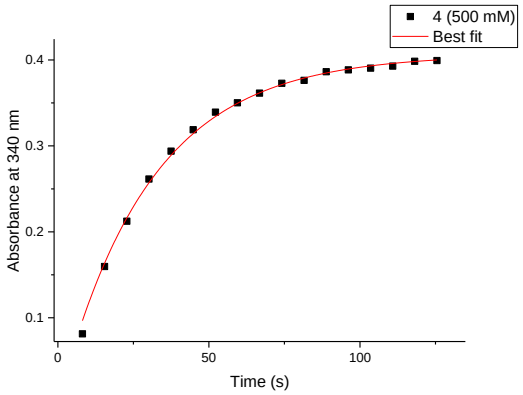

Representative time-resolved absorbance changes with best fits for the model reaction in saline at pH 4.5, 5.5, 6.5, 8.2, or 9.0 with various buffers at 50 mM (resulting values are listed in Table S3)

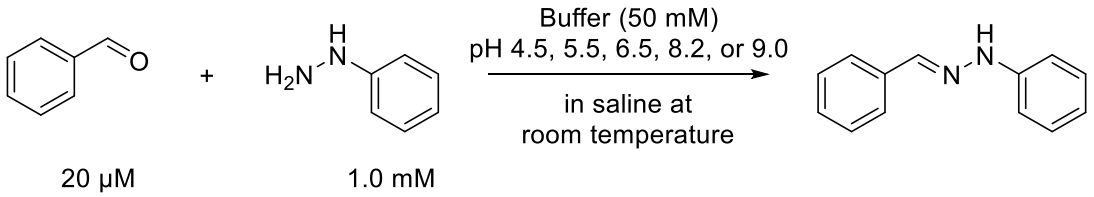

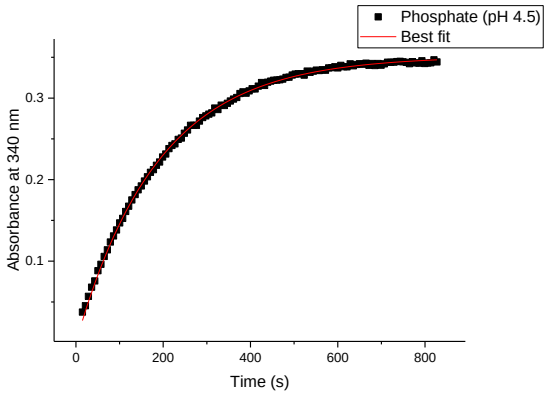

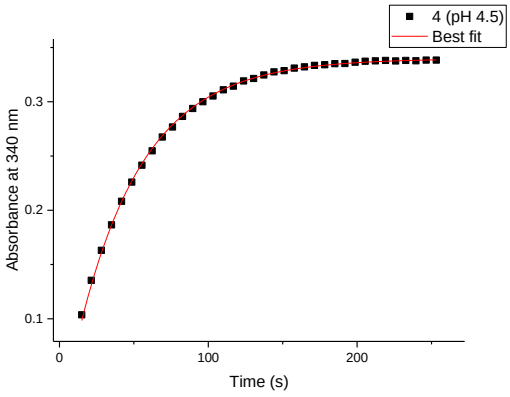

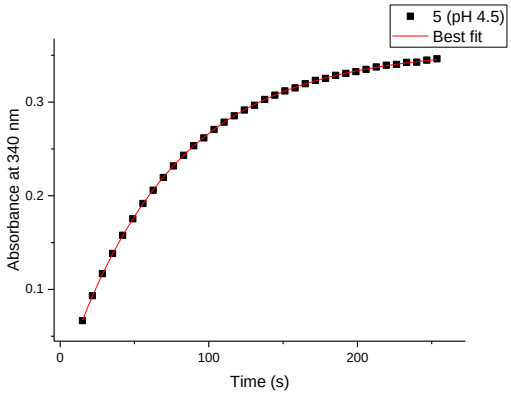
5 (pH 4.5)
Best fit
Absorbance at 340 nm
Time (s)

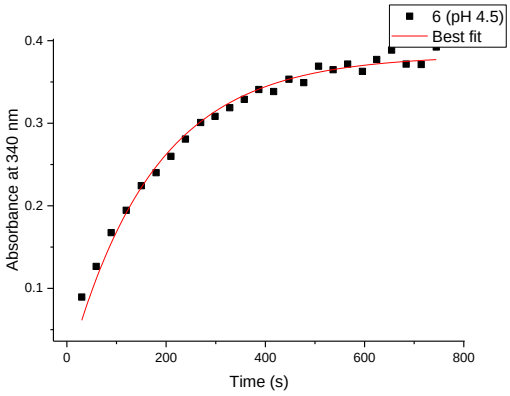
6 (pH 4.5)
Best fit
Absorbance at 340 nm
Time (s)

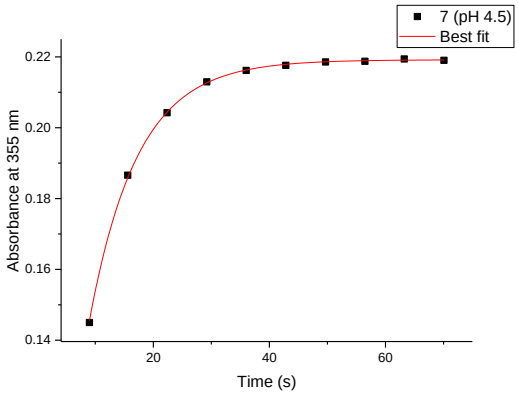
7 (pH 4.5)
Best fit
Absorbance at 355 nm
Time (s)

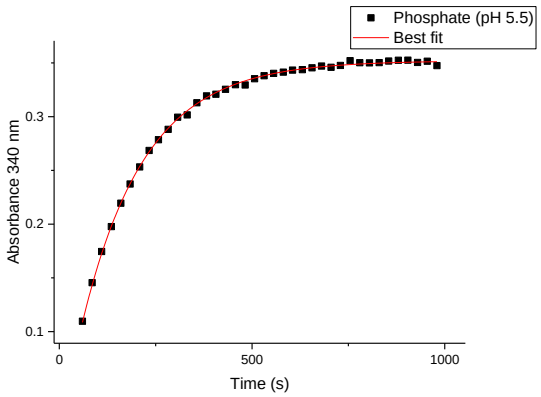
Phosphate (pH 5.5)
Best fit
Absorbance 340 nm
Time (s)

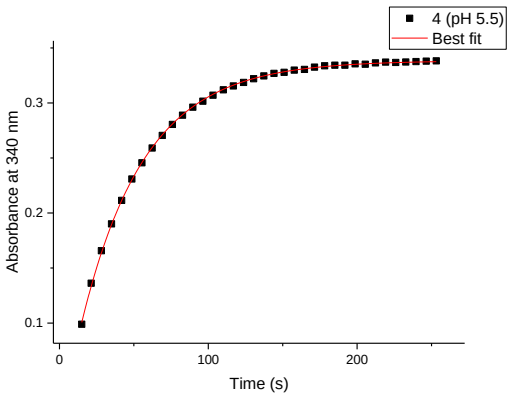
4 (pH 5.5)
Best fit
Absorbance at 340 nm
Time (s)

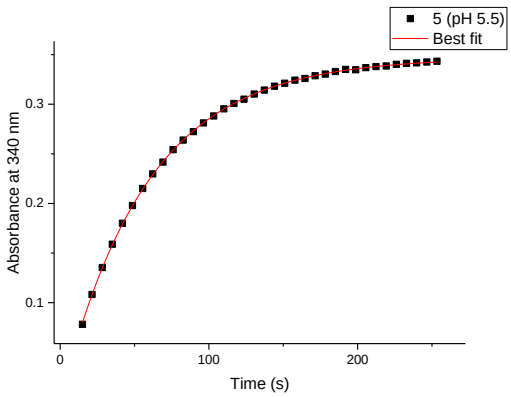
5 (pH 5.5)
Best fit
Absorbance at 340 nm
Time (s)

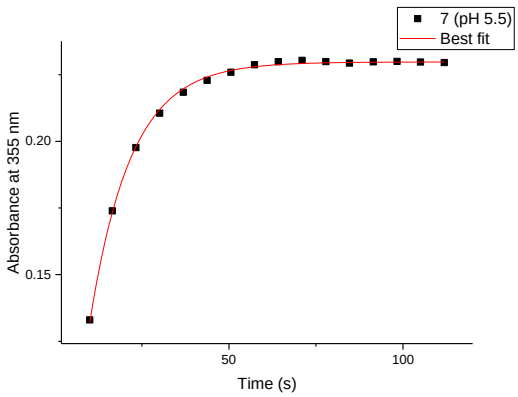
7 (pH 5.5)
Best fit
Absorbance at 355 nm
Time (s)

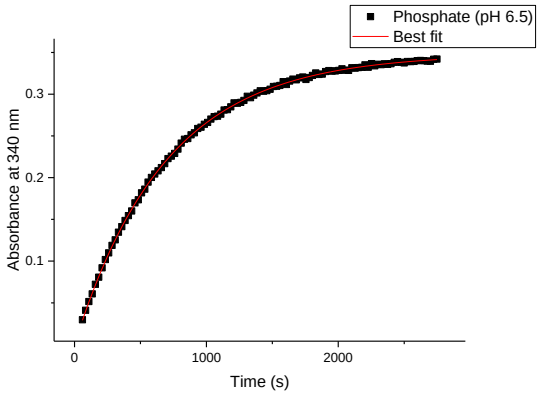
Phosphate (pH 6.5)
Best fit
Absorbance at 340 nm
Time (s)

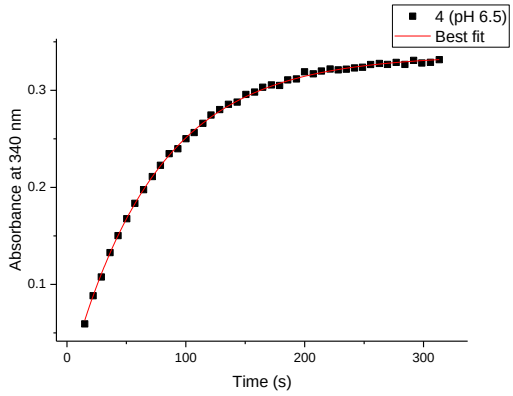
4 (pH 6.5)
Best fit
Absorbance at 340 nm
Time (s)

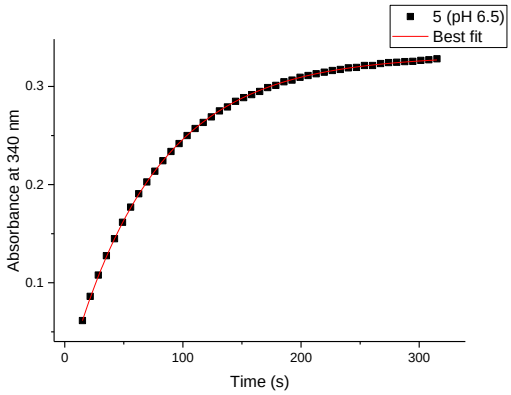
5 (pH 6.5)
Best fit
Absorbance at 340 nm
Time (s)

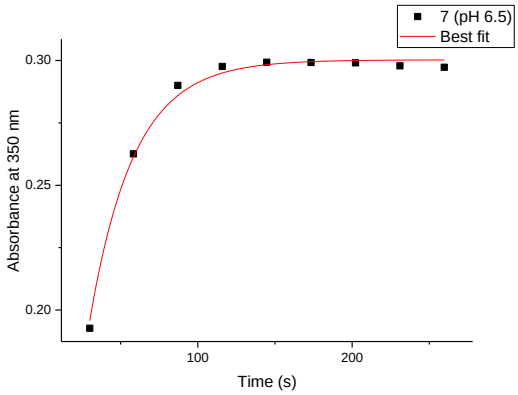
7 (pH 6.5)
Best fit
Absorbance at 350 nm
Time (s)

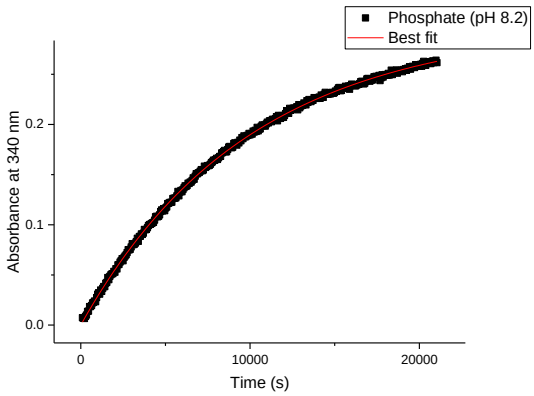
Phosphate (pH 8.2)
Best fit
Absorbance at 340 nm
Time (s)

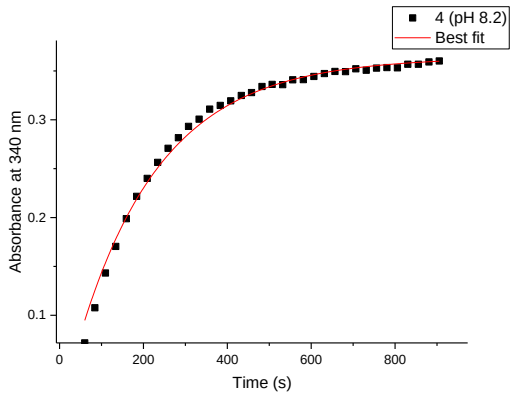
4 (pH 8.2)
Best fit
Absorbance at 340 nm
Time (s)

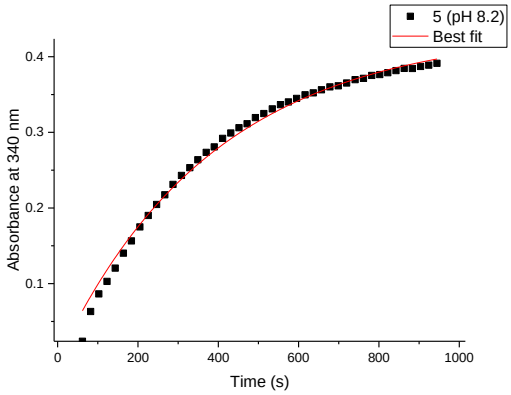
5 (pH 8.2)
Best fit
Absorbance at 340 nm
Time (s)

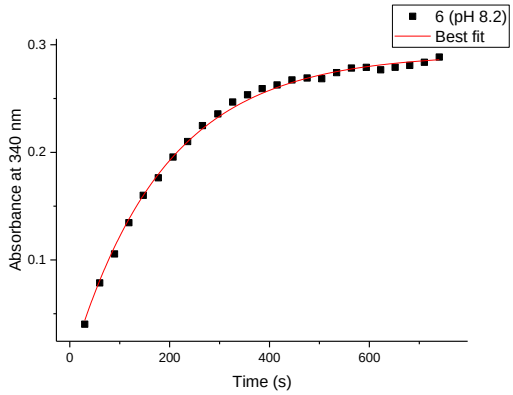
6 (pH 8.2)
Best fit
Absorbance at 340 nm
Time (s)

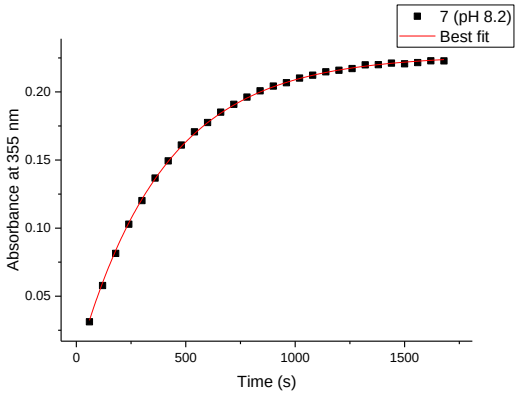
7 (pH 8.2)
Best fit
Absorbance at 355 nm
Time (s)

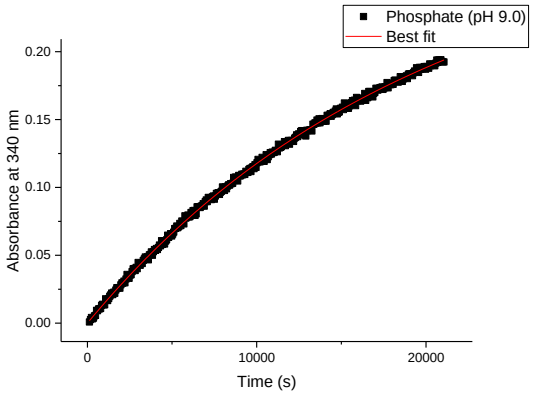
Phosphate (pH 9.0)
Best fit
Absorbance at 340 nm
Time (s)

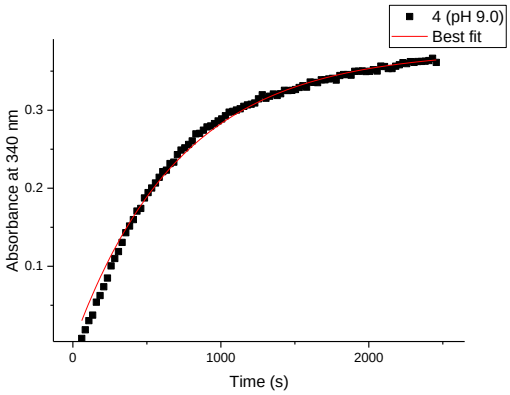
4 (pH 9.0)
Best fit
Absorbance at 340 nm
Time (s)

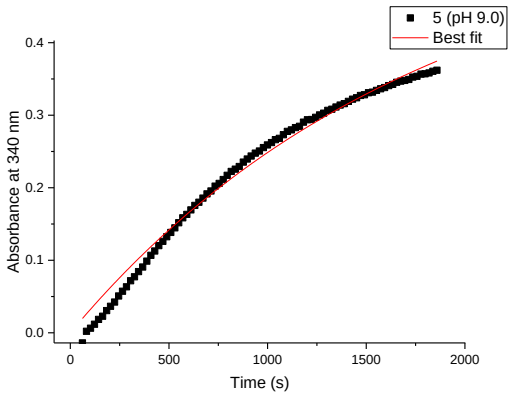
5 (pH 9.0)
Best fit
Absorbance at 340 nm
Time (s)

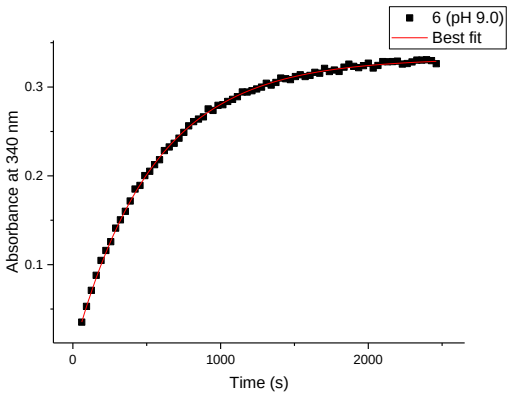
6 (pH 9.0)
Best fit
Absorbance at 340 nm
Time (s)

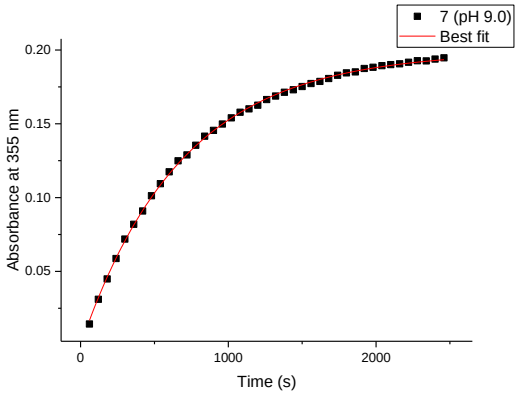
7 (pH 9.0)
Best fit
Absorbance at 355 nm
Time (s)

LC-MS analysis of reaction mixture:

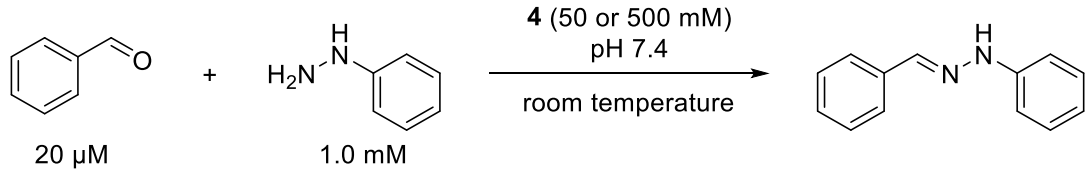

To ensure that stable Schiff-bases (or stable aminal/hemi-aminal) of the ABC and the aldehyde is not limiting the extent of hydrazone formation under the kinetic experiments, the reaction of benzaldehyde and phenylhydrazine in **4**-buffered water was monitored by LC-MS.

To **4**-buffered water (50 mM, pH 7.4) with benzaldehyde (20 µM) was added phenylhydrazine (1 mM). Chromatographic analysis of the reaction was carried out before addition of phenylhydrazine and ca. 20 min after addition, where the reaction has reached completion (Figure S9, A and B). Analysis of a solution of benzaldehyde in **4**-buffered water (50 mM, pH 7.4) showed no appreciable decomposition of benzaldehyde (Figure S9, C), supporting that the benzaldehyde conversion is caused by the addition of phenylhydrazine. Identical results (Figure S9, D-F) were obtained at higher buffer concentration (500 mM), supporting that even at 500 mM of **4**, no stable Schiff-bases prevents the full conversion into the hydrazone product.

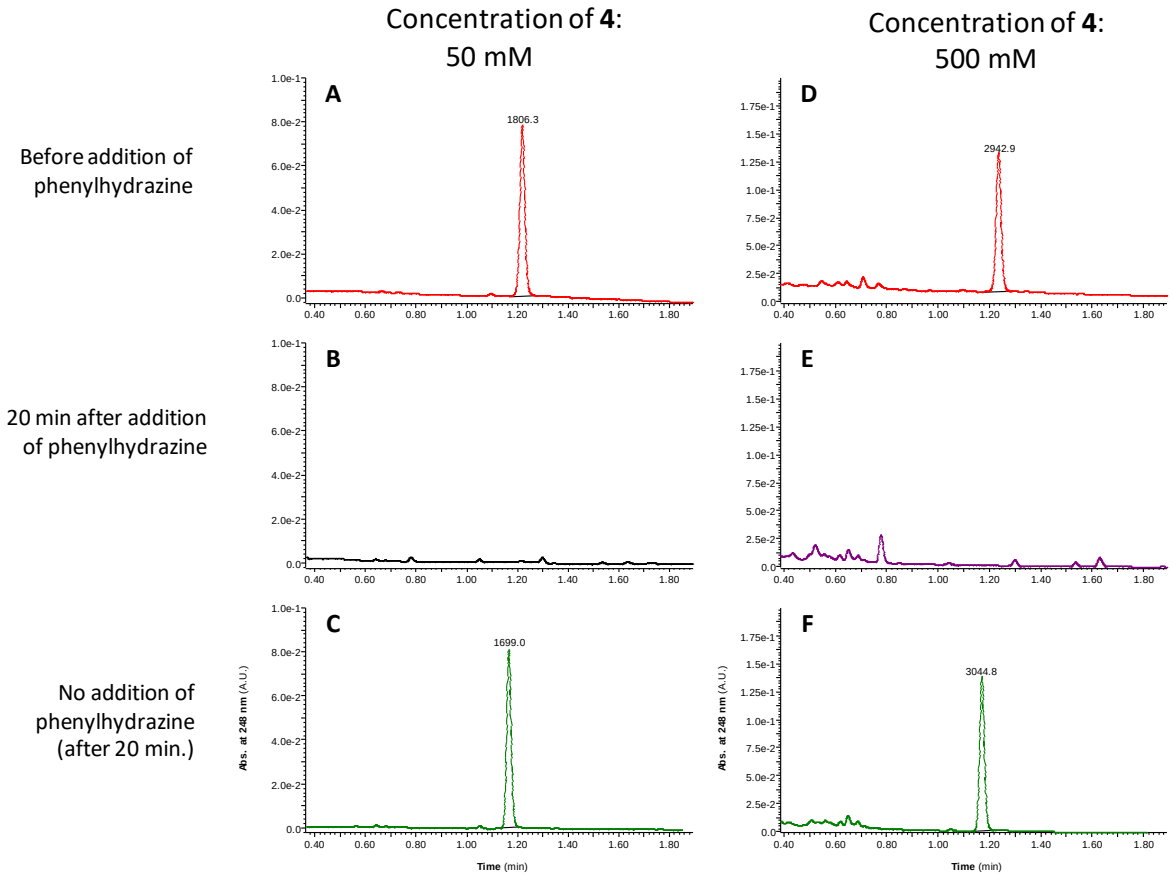

Figure S9: UPLC chromatograms (248 nm) of reaction mixture. Benzaldehyde section of chromatogram in 50/500 mM **4**-buffered water at pH 7.4 (A/D) before addition of phenylhydrazine; (B/E) Ca. 20 minutes after addition of phenylhydrazine; (C/F) after standing without phenylhydrazine for ca. 20 minutes.

Synthetic procedures

General procedures for organic synthesis:

Reagents and solvents were bought from commercial vendors and used as received, unless otherwise stated. Dry THF, toluene, MeCN, DCM and CCl_4 were bought as anhydrous grade and used without further purification. Reactions were monitored by thin-layer chromatography (TLC) carried out on 0.25 mm Merck silica gel plates (60–F_{254}) using a mercury vapor UV-lamp and basic $KMnO_4$[7] to visualize the analytes. Silica gel (particle size 40-63mm) was used for flash column chromatography.
NMR spectra were recorded on samples dissolved in either $CDCl_3$ or CD_3OD using a Varian Inova 500 MHz (126 MHz for ^{13}C) spectrometer. Residual undeuterated solvent was used as internal reference: $CHCl_3$ (^1H: δ = 7.26 ppm, ^{13}C: δ = 77.16 ppm), CD_2HOD (^1H δ = 3.31 ppm, ^{13}C δ = 49.00 ppm). The following abbreviations, or a combination thereof, were used to characterize the multiplicities: s = singlet, d = doublet, t = triplet, q = quartet, m = multiplet, br = broad.
HRMS analyses were performed on a Waters Acquity UPLC and Thermo Exactive Orbitrap mass spectrometer using electrospray ionization. Samples were introduced using Direct Injection with 100% MeOH as the carrier solvent. The flow rate was 0.2 mL/min, and the injection volume was 2 µL. Data was collected in full scan MS mode with a mass range of 100-1600 Da, Ultra High Resolution and Ultimate Mass Accuracy settings.

2-Iodo-4,5-dimethylaniline

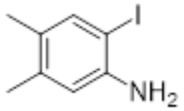

To a 1 L round bottom flask equipped with a magnetic stirring bar was transferred 4,5-dimethylaniline (12.2 g, 0.1 mol) and $NaHCO_3$ (25.2 g, 0.3 mol). DCM/H_2O (667 mL, 2:1) was added to the solids and the reaction vessel was sealed. Argon was bubbled through the mixture for 15 min while stirring. Iodine (25.4 g, 0.1 mol) was transferred to the reaction vessel and argon was bubbled through for additional 30 min while stirring. The reaction mixture was then stirred under an atmosphere of argon for 26 h. The layers of the biphasic system were separated and the aqueous phase was extracted with DCM (200 mL). The organic layers were combined, washed with $Na_2S_2O_3$ (200 mL, sat. aq./H_2O 1:3), dried over $MgSO_4$, filtered and concentrated under reduced pressure to a brown solid (23.9 g, 97%); R_f (DCM) = 0.55; ^1H NMR (500 MHz, $CDCl_3$) δ 7.41 (s, 1H), 6.58 (s, 1H), 3.88 (br s, 2H), 2.16 (s, 3H), 2.14 (s, 3H); ^{13}C NMR (126 MHz, $CDCl_3$) δ 144.60, 139.06, 137.96, 128.61, 116.33, 80.61, 19.61, 18.36; HRMS calcd for $C_8H_{11}IN$ [M + H] 247.9931, found 247.9928.

Diethyl (2-amino-4,5-dimethylphenyl)phosphonate

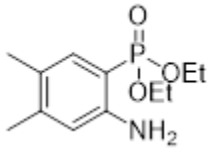

An oven-dried 500 mL round bottom flask equipped with a magnetic stirring bar was sealed and cooled to room temperature under vacuum. The flask was refilled with argon and thereafter charged with 2-iodo-4,5-dimethylaniline (12.4 g, 50.0 mmol) and K_2CO_3 (13.8 g, 100.0 mmol). The atmosphere was evacuated and the flask was refilled with argon (2 cycles). Dry toluene (125 mL), diethyl phosphite (8.37 mL, 65 mmol)

and N,N'-dimethylethylenediamine (1.08 mL, 10 mmol) were transferred to the flask and argon was bubbled through the mixture for 30 min while stirring. Finally, CuI (480 mg, 2.5 mmol) was added and argon was bubbled through the mixture for additional 15 min while stirring. The mixture was then heated to 100°C and stirred at that temperature for 18 h. After being cooled to rT, H_2O (150 mL) was transferred to the reaction flask and the resulting phases were separated. The aqueous phase was extracted with EtOAc (2 × 150 mL), the organic layers were combined, dried over $MgSO_4$, filtered and concentrated under reduced pressure to a dark brown liquid. The crude product was purified by column chromatography (ø = 9 cm, petroleum ether/EtOAc 1:1 → 1:4) to yield the product as a light tan oil (6.96 g, 54%); R_f (EtOAc) = 0.4; ^{1}H NMR (500 MHz, $CDCl_3$) δ 7.19 (d, *J* = 14.3 Hz, 1H), 6.50 (d, *J* = 6.8 Hz, 1H), 4.79 (br s, 2H), 4.18 – 4.08 (m, 2H), 4.07 – 3.98 (m, 2H), 2.18 (s, 3H), 2.14 (s, 3H), 1.32 (td, *J* = 7.1, 0.6 Hz, 6H); ^{13}C NMR (126 MHz, $CDCl_3$) δ 149.32 (d, *J* = 8.2 Hz), 143.35 (d, *J* = 2.7 Hz), 133.35 (d, *J* = 7.9 Hz), 125.20 (d, *J* = 14.0 Hz), 117.51 (d, *J* = 13.4 Hz), 105.11 (d, *J* = 184.9 Hz), 61.74 (d, *J* = 4.9 Hz), 20.04, 18.54, 16.26 (d, *J* = 6.8 Hz); HRMS calcd for $C_{12}H_{21}NO_3P$ [M + H] 258.1254, found 258.1249.

Diethyl (2-acetamido-4,5-dimethylphenyl)phosphonate

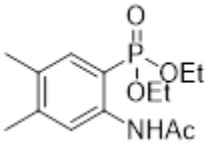

An oven-dried 50 mL round bottom flask equipped with a magnetic stirring bar was sealed and cooled to room temperature under vacuum. The flask was refilled with argon and diethyl (2-amino-4,5-dimethylphenyl)phosphonate (3.1 g, 12 mmol) was thereafter transferred to it. The atmosphere was evacuated and the flask was refilled with argon (3 cycles). Ac_2O (12 mL) was transferred to the reaction vessel and the resulting solution was stirred at room temperature for 60 min, after which H_2O (25 mL) was added to quench the reaction. The mixture was stirred for 2 h and thereafter diluted with EtOAc (300 mL). The organic layer was washed with H_2O (150 mL) and brine (150 mL), dried over $MgSO_4$, filtered and concentrated under reduced pressure in a rotary evaporator. The obtained residue was left under high vacuum for 7 days, yielding the product as a light brown crystalline solid of sufficient purity to be used in the next step (3.4 g, 95%); ^{1}H NMR (500 MHz, $CDCl_3$) δ 10.39 (br s, 1H), 8.35 (d, *J* = 6.8 Hz, 1H), 7.26 (d, *J* = 14.5 Hz, 1H), 4.17 – 4.06 (m, 2H), 4.06 – 3.97 (m, 2H), 2.28 (s, 3H), 2.21 (s, 3H), 2.17 (s, 3H), 1.31 (td, *J* = 7.1, 0.6 Hz, 6H); ^{13}C NMR (126 MHz, $CDCl_3$) δ 169.02, 143.84, 140.75, 132.86 (d, *J* = 6.5 Hz), 131.72 (d, *J* = 13.8 Hz), 121.98 (d, *J* = 12.2 Hz), 110.56 (d, *J* = 181.1 Hz), 62.59 (d, *J* = 5.1 Hz), 25.29, 20.57, 19.28, 16.32 (d, *J* = 6.8 Hz); HRMS calcd for $C_{14}H_{23}NO_4P$ [M + H] 300.1359, found 300.1357.

Diethyl (2-acetamido-5-((dimethylamino)methyl)-4-methylphenyl)phosphonate

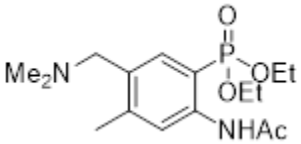

Diethyl (2-acetamido-4,5-dimethylphenyl)phosphonate (1.8 g, 6 mmol) was transferred to an oven-dried 50 mL round bottom flask equipped with a magnetic stirring bar. The flask was left under high vacuum for 6 days and thereafter refilled with argon. The reaction vessel was charged with NBS (1.0 g, 5.7 mmol) and benzoyl peroxide (73 mg, 0.3 mmol), equipped with a cooler and sealed. The atmosphere was evacuated and the flask was refilled with argon (3 cycles). Dry CCl_4 (12 mL) was transferred to it and the resulting

mixture was heated to reflux and stirred for 8 h. After allowing the mixture to cool to room temperature, solid succinimide was filtered off. The reaction vessel was rinsed with EtOAc (5 mL) at -78°C and the resulting mixture was used to wash the filtercake. The combined solutions were concentrated under reduced pressure to leave a brown oil (2.2 g). The obtained oil was left in a 100 mL round bottom flask equipped with a magnetic stirring bar under high vacuum for 3 days. The flask was sealed and flushed with argon for 10 min. The residue was dissolved in dry THF (6 mL), whereafter dimethyl amine (18 mL, 2M in THF) was transferred over 5 min while stirring. Precipitate was observed immediately. The mixture was stirred at rT for 60 min, diluted with EtOAc (300 mL), washed with NaOH (2 × 50 mL, 1M, aq.) and brine (50 mL). The organic layer was dried over $MgSO_4$, filtered and concentrated under reduced pressure to a brown oil. The residue was purified by column chromatography (ø = 4 cm, DCM/MeOH/NH_4OH (conc., aq.) 100:0:0 → DCM/MeOH/NH_4OH (conc., aq.) 100:2:0 → DCM/MeOH/NH_4OH (conc., aq.) 100:5:1) to yield the product as a light tan oil (792 mg, 72%); The amine position was confirmed by NOESY (see attached spectrum for analysis); R_f (DCM/MeOH 9:1) = 0.3; ^{1}H NMR (500 MHz, $CDCl_3$) δ 10.50 (br s, 1H), 8.38 (d, *J* = 6.7 Hz, 1H), 7.37 (d, *J* = 14.7 Hz, 1H), 4.13 – 4.03 (m, 2H), 4.03 – 3.93 (m, 2H), 3.28 (s, 2H), 2.35 (s, 3H), 2.16 (s, 6H), 2.15 (s, 3H), 1.30 – 1.25 (m, 6H); ^{13}C NMR (126 MHz, $CDCl_3$) δ 169.08, 144.90, 141.90 (d, *J* = 7.7 Hz), 133.55 (d, *J* = 6.6 Hz), 132.42 (d, *J* = 13.6 Hz), 122.40 (d, *J* = 11.9 Hz), 110.25 (d, *J* = 180.9 Hz), 62.69 (d, *J* = 5.0 Hz), 61.58, 45.59, 25.50, 20.01, 16.44 (d, *J* = 6.7 Hz); HRMS calcd for $C_{16}H_{28}N_2O_4P$ [M + H] 343.1781, found 343.1782.

*(2-Amino-5-((dimethylamino)methyl)-4-methylphenyl)phosphonic acid dihydrobromide (**18**)*

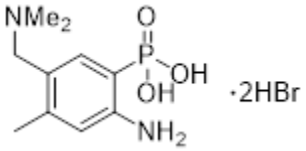

To a 25 mL round bottom flask equipped with a magnetic stirring bar was transferred diethyl (2-acetamido-5-((dimethylamino)methyl)-4-methylphenyl)phosphonate (496 mg, 1.45 mmol). H_2O (1.5 mL) was transferred to the reaction vessel and stirring was initiated. HCl (1.5 mL, 12 M, aq.) was thereafter transferred dropwise and the resulting mixture was stirred at rT for 48 h. The reaction was quenched by slow addition of NaOH (50 mL, 1 M, aq.) and thereafter diluted further with brine (25 mL) and extracted with EtOAc (3 × 100 mL). The combined extracts were dried over $MgSO_4$, filtered and concentrated to a light-yellow oil. Hydrolysis of the acetamide functionality was confirmed by ^{1}H-NMR. The oil was transferred to a 100 mL round bottom flask equipped with a magnetic stirring bar and dried under high vacuum for a night. The flask was flushed with argon for 10 min and dry MeCN (11.8 mL) was thereafter transferred to it. To the yellow solution, TMSBr (1.4 mL, 10.6 mmol) was dropwise added while stirring. The solution was stirred at rt for 24 h and volatiles were thereafter removed using a rotary evaporator, leaving an orange crystalline solid. The solid residue was left under high vacuum for a night and subsequently washed with EtOAc (3 × 5 mL). The solid was thereafter dissolved in MeOH (5 mL) and concentrated under reduced pressure to remove residual TMSBr and hydrolyze any remaining phosphonate silyl esters. The MeOH treatment was repeated twice. The obtained hygroscopic orange crystals were dried under high vacuum for a night (560 mg, 103%). The presence of bromide was validated by MS. ^{1}H NMR (500 MHz, CD_3OD) δ 7.57 (d, *J* = 14.8 Hz, 1H), 6.73 (d, *J* = 6.1 Hz, 1H), 4.26 (s, 2H), 2.86 (s, 6H), 2.37 (s, 3H); ^{13}C NMR (126 MHz, CD_3OD) δ 149.71, 144.95, 138.06, 120.57 (d, *J* = 10.4 Hz), 119.63 (d, *J* = 13.5 Hz), 115.07 (d, *J* = 185.9 Hz), 59.12, 42.85, 19.94; HRMS calcd for $C_{10}H_{18}N_2O_3P$ [M + H] 245.1050, found 245.1049.

Supporting References

1. R. de Levie, *The Chemical Educator*, 1996, **1**, 1.
2. C. C. Price and H. Kroll, *J. Am. Chem. Soc.*, 1938, **60**, 2726.
3. W. Y. Kim, H. Shi, H. S. Jung, D. Cho, P. Verwilst, J. Y. Lee and J. S. Kim, *Chem. Commun.*, 2016, **52**, 8675.
4. P. Crisalli, A. R. Hernández and E. T. Kool, *Bioconjugate Chem.*, 2012, **23**, 1969.
5. L. H. Yuen, N. S. Saxena, H. S. Park, K. Weinberg and E. T. Kool, *ACS Chem. Biol.*, 2016, **11**, 2312.
6. D. Chelius and T. A. Shaler, *Bioconjugate Chem.*, 2003, **14**, 205.
7. L. Cai, in *Current Protocols Essential Laboratory Techniques*, Editon edn., 2014, pp. 6:6.3:6.3.1–6.3.18.